Galaxies

Pierluigi Monaco,

Radiative Processes

2018/2019

From dustpedia.org

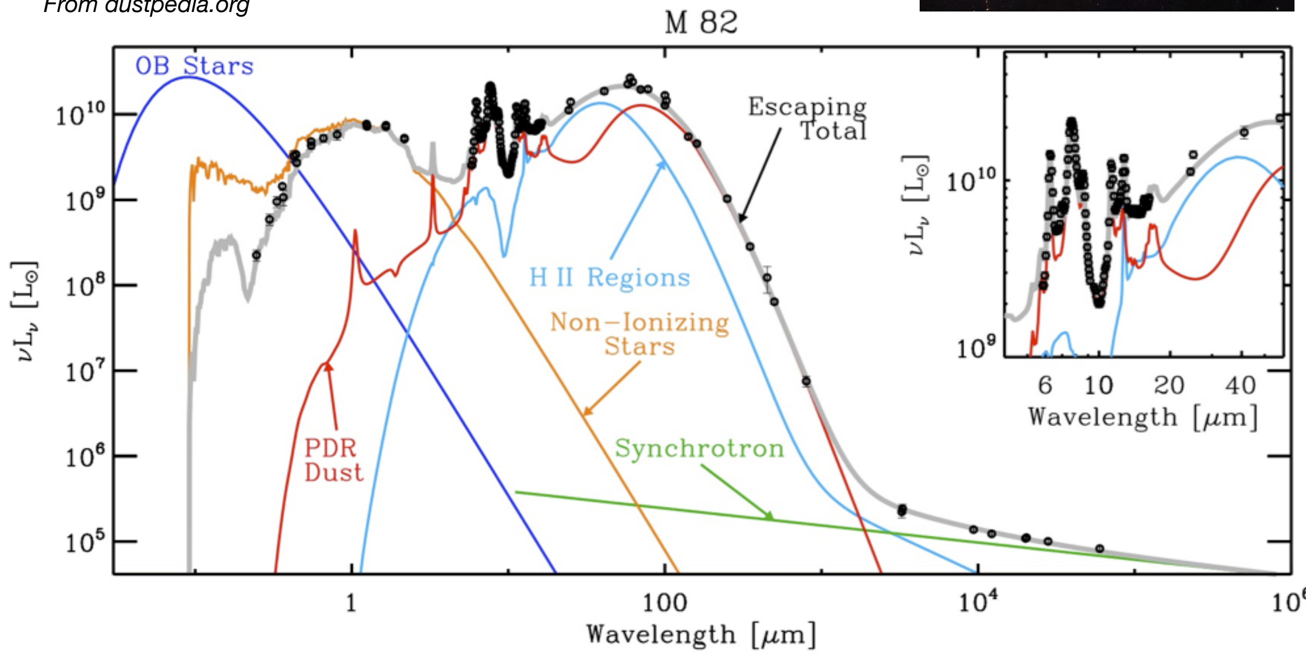

This slide shows the SED of the starburst galaxy M82 (top right), black points are data, colored lines give the various components of a model (that will be illustrated below), the gray line is the fit to the data.

From stellar spectra to galaxy SEDs

These slides illustrate how to go from the spectral energy distributions (SEDs) of stars to those of galaxies.

Needed ingredients:

Stellar spectra libraries

Stellar evolution models

Stellar Initial Mass Function (IMF)

Star Formation Rate - SFR(t)

Gas metallicity Z(t)

un-extincted stellar light

of

and of non-ionizing stars

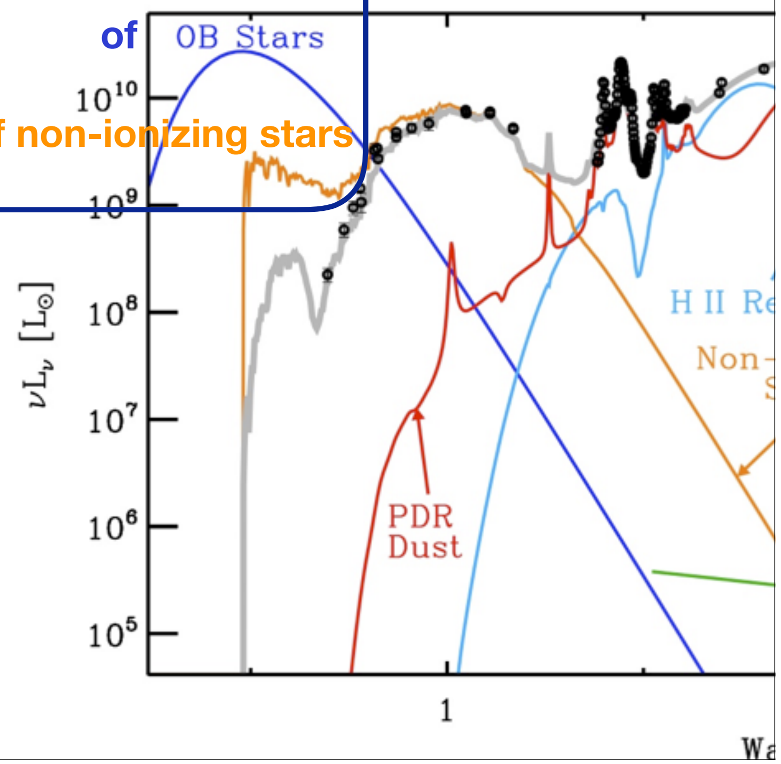

To synthetise the SED of a realistic stellar population, without dust extinction, you need libraries of stellar SEDs, stellar evolution models, an assumption on the stellar Initial Mass Function (IMF), the galaxy Star Formation Rate (SFR) and the evolution of gas metallicity Z(t) with time (this is the same of the metallicity of newly born stars).

SED of a Simple Stellar Population (SSP)

An SSP is a population of stars that share the same age and metallicity.

A star cluster may be a good example of SSP - with the exception of the early evolution phases, where the little age differences between stars can be important.

Parameters are:

- (luminosities scale with) mass,
- stellar age,
- stellar metallicity,
- stellar IMF,

plus:

- spectral libraries,
- stellar tracks.

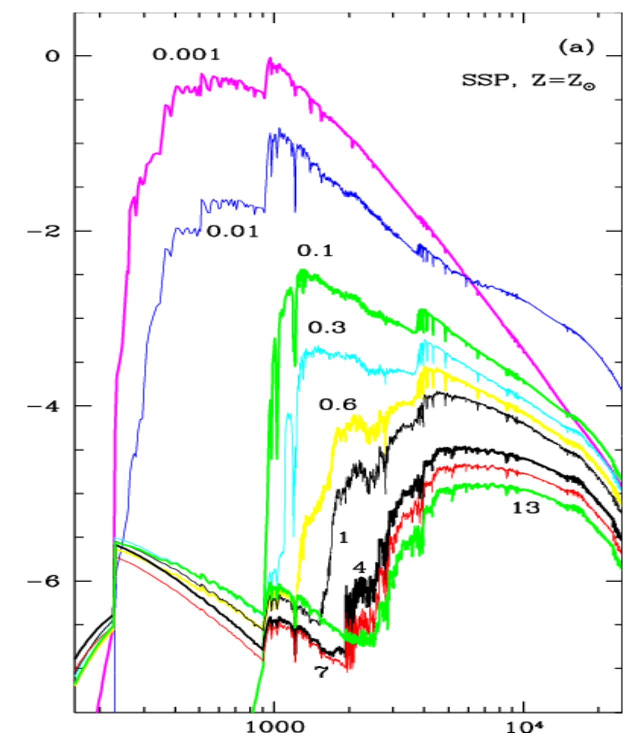

From Bruzual (2000)

This slide illustrates how to compute the SED of a Simple Stellar Population (SSP). The figure gives examples of SSP SEDs for a constant metallicity and varying age (in Gyr).

SED of a Simple Stellar Population (SSP)

An SSP is a population of stars that share the same age and metallicity.

A star cluster may be a good example of SSP - with the exception of the early evolution phases, where the little age differences between stars can be important.

Parameters are:

- (luminosities scale with) mass,
- stellar age,
- stellar metallicity,
- stellar IMF,

plus:

- spectral libraries,
- stellar tracks.

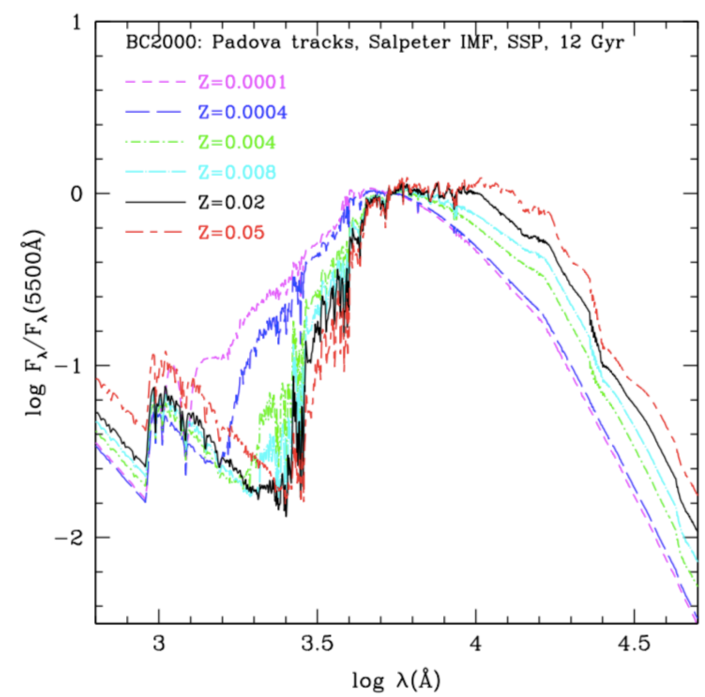

From Bruzual (2000)

The figure here gives SSP SEDs with constant age of 12 Gyr and varying metallicity.

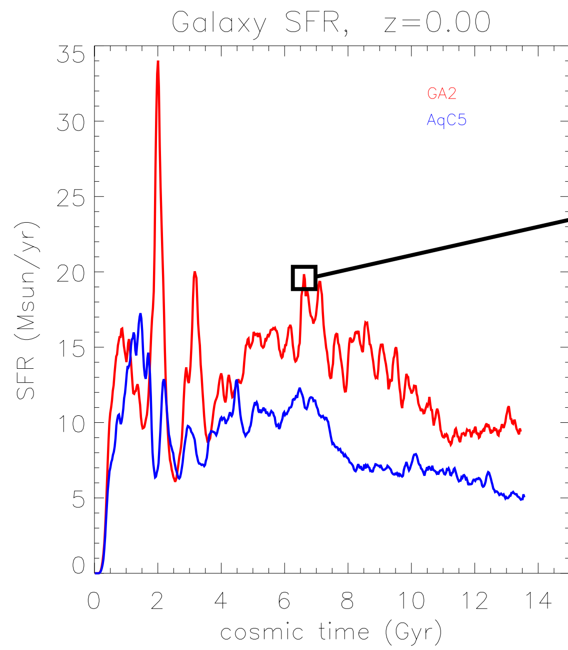

SED of a stellar population with a complex SFR(t)

Stars formed in a time interval are treated like an SSP

as an example,
SFR of a simulated galaxy,
Murante et al. (2015)

$$L_\nu = \int_o^{t_0} dt\ SFR(t)\ L_\nu^{(\mathrm{SSP,1\,M_\odot})}(t_0 - t, Z_{\mathrm{gas}}(t))$$

$$L_\nu^{(\mathrm{SSP,1\,M_\odot})}(t_0 - t, Z_{\mathrm{gas}}(t)) = \mathrm{const} \times \int_{m_l}^{m_u} dm\ \boxed{\phi(m)}\ L_\nu^{\mathrm{star}}(m, t_0 - t, Z)$$

IMF

This slide illustrates how to go from SSP SEDs to the SED of a complex population with time-dependent SFR and Z. Binning the SFR in time, each little contribution to the SFR can be modeled as an SSP. The SSP SED (lower formula) is an integral of the stellar SEDs at given time (t_0 is the age of the universe) weighted by the stellar IMF, the galaxy SED is an integral of the SSP SEDs weighted by the SFR.

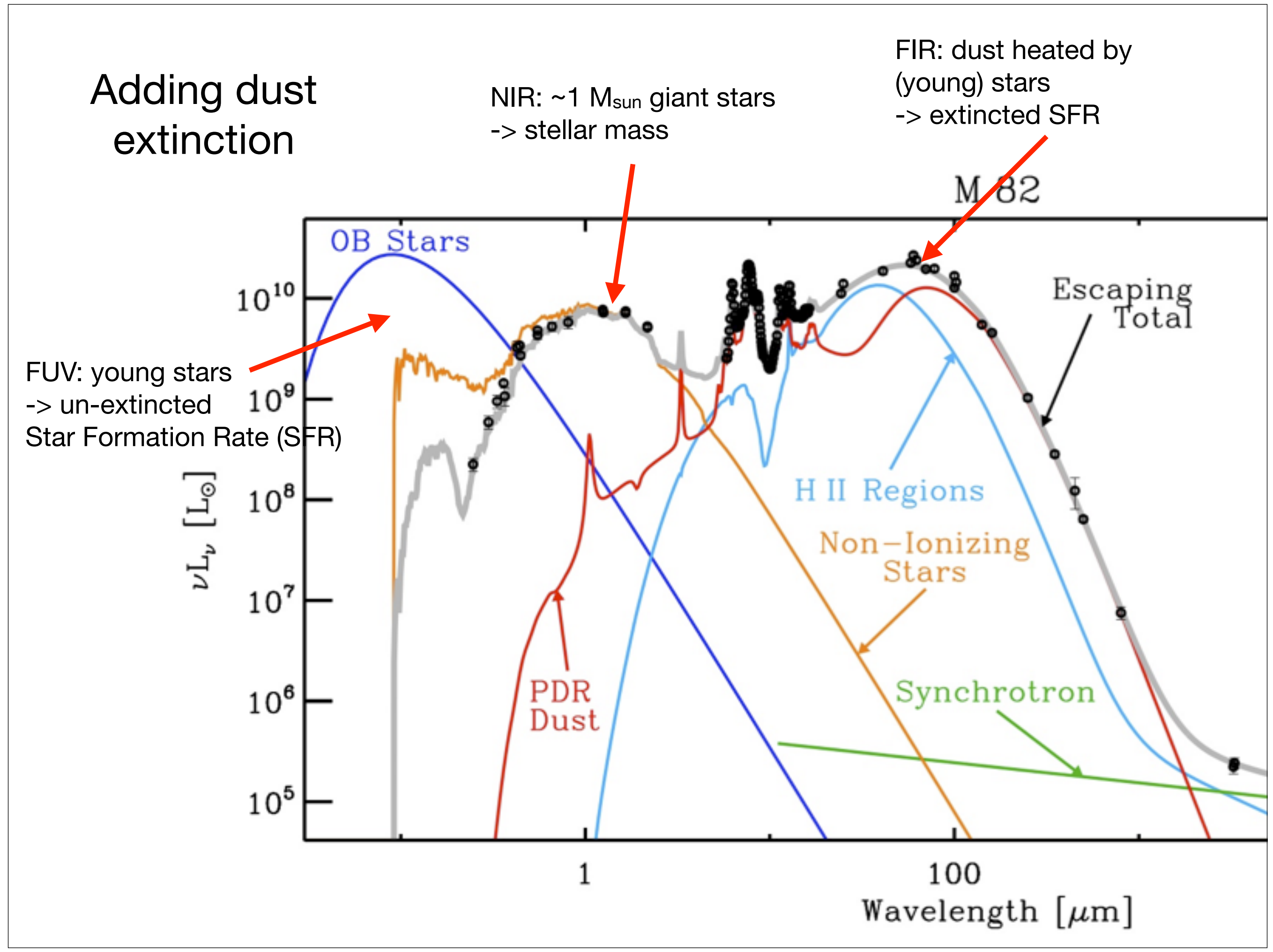

When dust extinction is added, FUV light is absorbed and re-emitted in the FIR (see the lecture by G. Granato). The SED is very sensitive to massive stars in the FUV, so it traces the unextincted SFR; the NIR is sensitive to the bulk of stellar mass, while FIR tracks the re-emission by dust of absorbed FUV energy, so it is sensitive to extincted SFR.

(Un-extincted) UV light

The 1500 A luminosity of an SSP drops quickly with time, especially after 3 x 10^8 yr.

For a constant SFR, the UV luminosity is constant after ~10^8 yr.

These numbers depend weakly on metallicity.

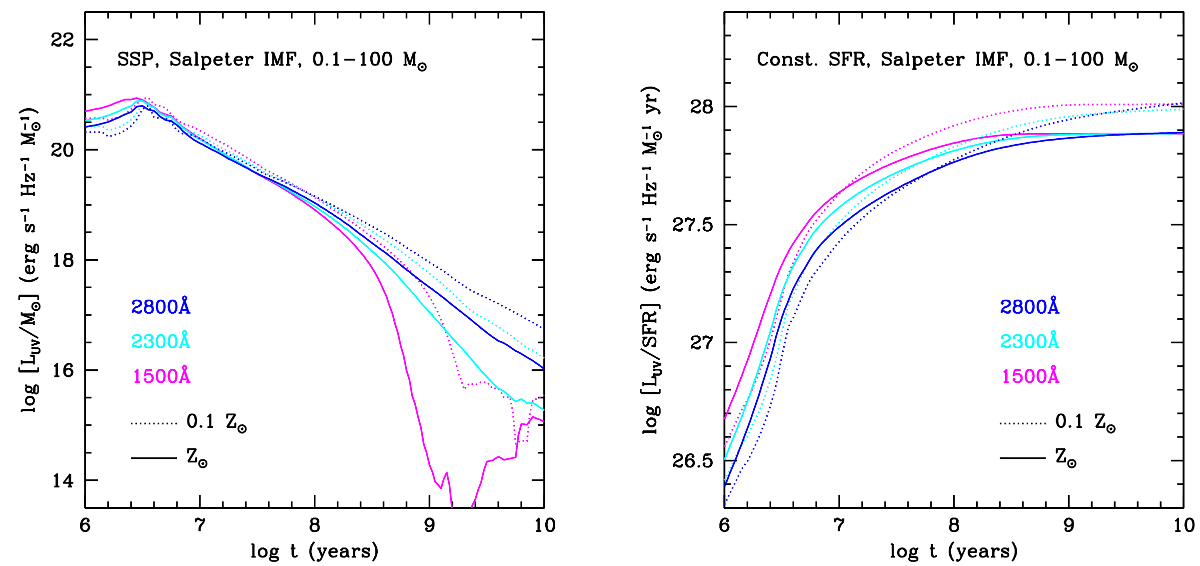

from Madau & Dickinson

These plots, taken from Madau & Dickinson, show the evolution of FUV luminosity in three bands in two cases: SSPs and stellar populations with constant SFR. The left figure is given in units of erg / s / Hz per solar mass, the right figure in erg / s / Hz per solar mass / yr, the units of measure of SFR.

From galaxy SEDs to physical quantities

These slides illustrate how to go from galaxy SEDs to physical quantities like stellar mass and SFR.

Star Formation Rate indicators

SFR is mainly calibrated on local molecular clouds by counting the number of "Young Stellar Objects", that is massive newly born (pre-main sequence) stars. If <*M*> is the total mass of new stars for each YSO and τ the YSO lifetime:

$$SFR = N_{\rm YSO} \frac{\langle M \rangle}{\tau}$$

Then light at a SFR-sensitive wavelength is correlated with this SFR.

The main SFR indicators are:

- UV (1500 A) luminosity,
- 24 μm luminosity,
- total IR luminosity, from 8 to 1000 μm,
- Hα line luminosity, emerging from HII regions,
- Paschen-α line luminosity, if observable,
- other nebular lines,
- radio luminosity,
- X-ray luminosity.

To account for dust extinction:

- correct UV data for extinction, using the (reddened) UV slope,
- add UV and FIR SFR indicators.

This slide describes the main SFR indicators, that can be used to estimate a galaxy SFR. It is important to know that the main calibration comes from counting Young Stellar Objects (massive protostars) in nearby molecular clouds of the Milky Way.

$$SFR = SFR_{\mathrm{UV}} + SFR_{\mathrm{IR}}$$

$$SFR_{\mathrm{UV}} = \kappa_{\mathrm{FUV}} \times L_{\nu}(FUV)$$

$$SFR_{IR} = \kappa_{\mathrm{FIR}} \times L_{\mathrm{IR}}$$

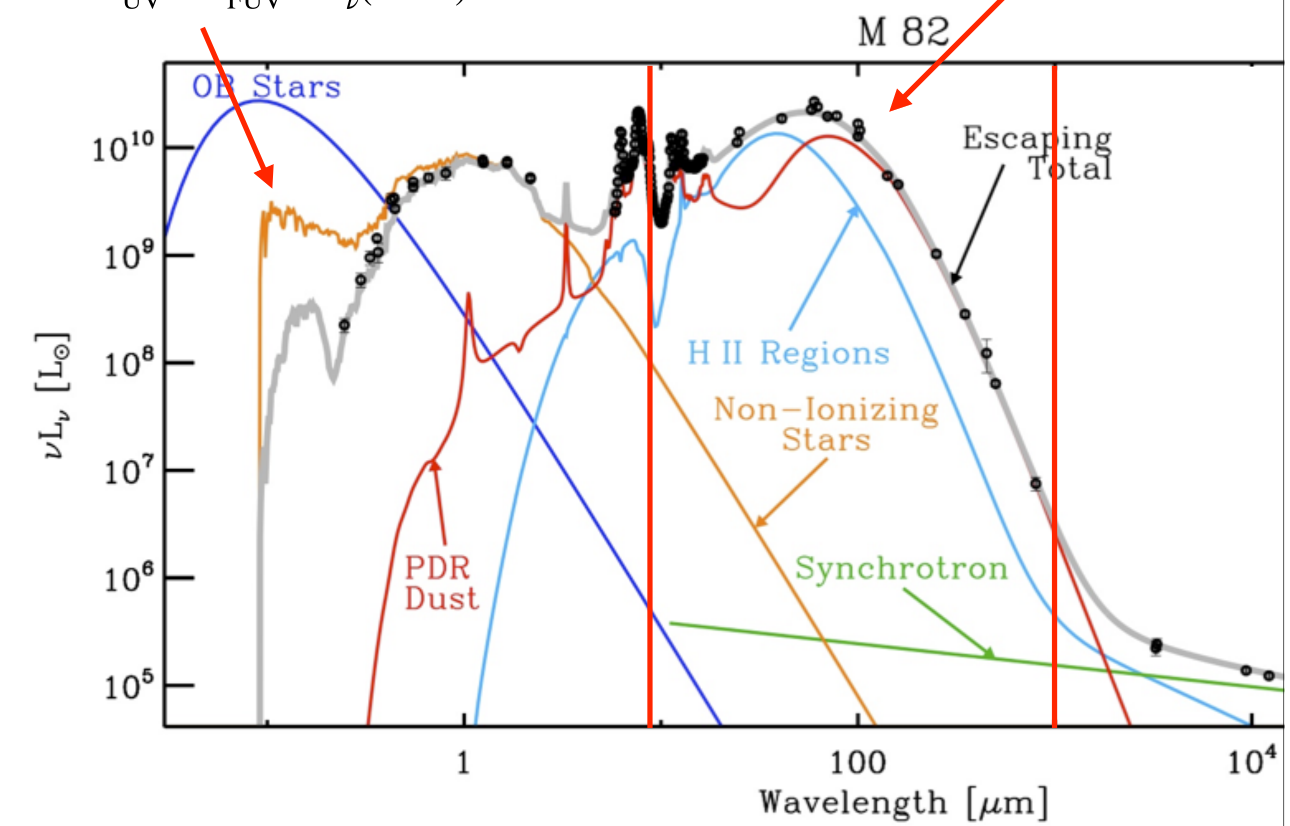

A very effective way to measure SFR is to sum the contributions from FUV and FIR, so as to measure both extincted and unextincted contributions. Here L_IR is the integrated luminosity from 8 to 1000 micron. Calibration constants are discussed in Madau & Dickinson.

Stellar mass measurements

- Luminosity in some red band (K band at 2 m, or Spitzer NIR bands)
- Average M/L in the K-band
- Correction for (little) extinction

FIGURE: M/L ratio for 12 Gyr SSP and different SSP SED libraries,

from Courteau et al 2014, Reviews of Modern Physics, vol. 86, Issue 1, pp. 47-119

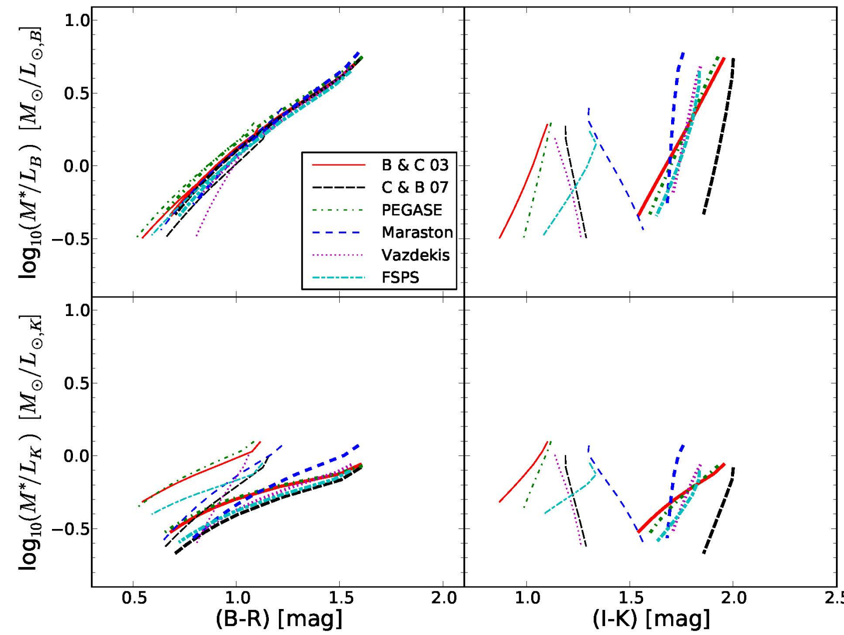

To measure stellar masses one needs to measure luminosity in some NIR band, ideally K-band from the ground or NIR bands at 3.6 or 4.5 micron from Spitzer satellite. The figure shows how the mass-to-light ratio in B and K bands varies with color for various SSPs (created by different authors) of 12 Gyr and varying metallicity. Notably, M/L does not vary much in the K-band, but is it not constant, meaning that the calibration from K-band to stellar mass is uncertain.

SED fitting

Main parameters:

- REDSHIFT!
- stellar mass
- Star Formation Rate, SFR(t_{obs})
- Star Formation Rate history, SFR(t)
- metallicity, Z(t_{obs})
- metallicity history Z(t)
- IMF
- extinction and reddening (dust mass and geometry)
- library of galaxy SEDs
- **AGN contamination**

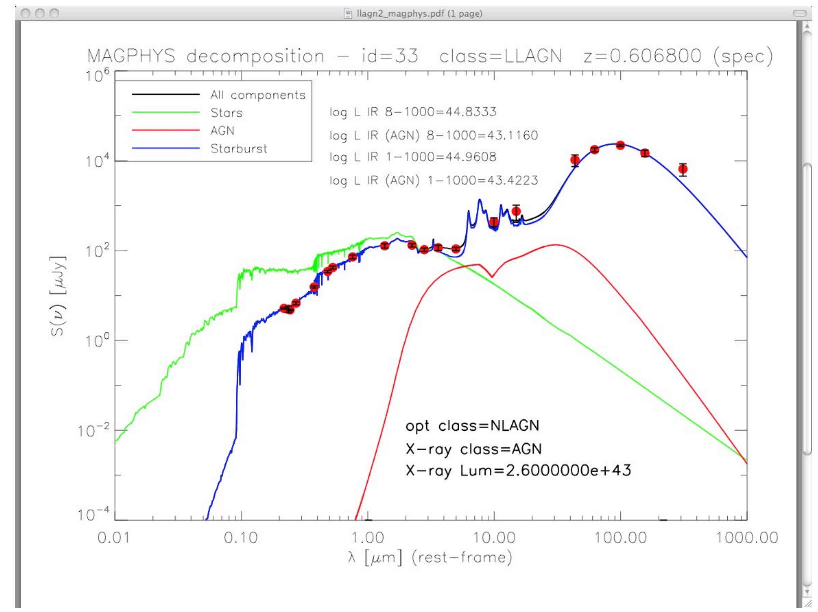

courtesy of C. Gruppioni

Another way to measure stellar masses, and not only those, is SED fitting: the broad-band SED of galaxies, obtained by taking images in several bands, is fit with a model, and this allows to fix model parameters listed in the slide, starting from redshift. However, and assumption on SFR(t) and on the metallicity history needs to be done, and contamination from an AGN component must be taken into account.

The Schmidt-Kennicutt relation

Measurement of the SFR applied to neaby galaxies reveals that the surface density of SFR is correlated with the gas surface density.

The Schmidt-Kennicutt relation

Estimating the SFR of a galaxy, it is possible to notice a correlation of surface densities of SFR and gas mass.

This was first noticed by Maarten Schmidt in 1959, then confirmed by several authors among which Robert Kennicutt.

With significant uncertainties, the relation has been fit as:

$$\Sigma_{\rm SFR} \propto \Sigma_{\rm gas}^{1.4}$$

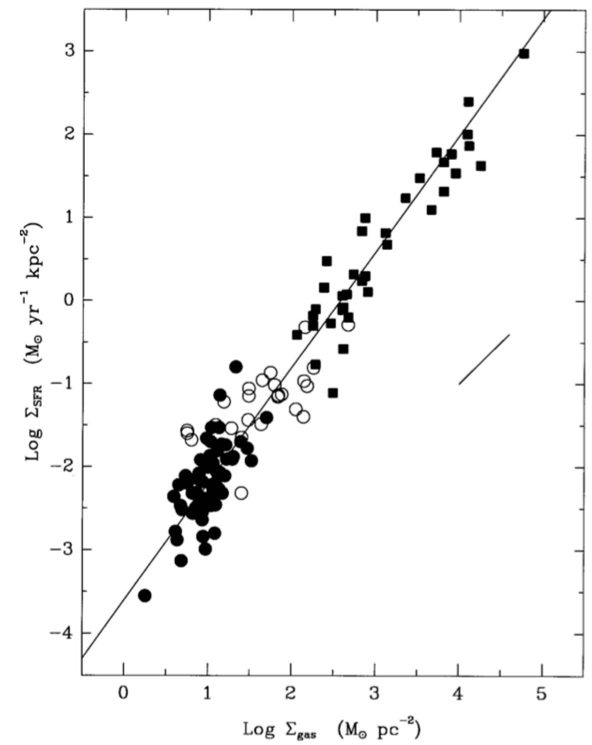

This slide describes the knowledge on this relation up to 2008. The segment in the plot gives a linear relation between the two quantities. Gas density was estimated using 21 cm line (neutral hydrogen) and C-O emission (molecular hydrogen).

The Schmidt-Kennicutt relation

A breakthrough was obtained in 2008 thanks to a suite of multiwavelength surveys of a sample of nearby spirals.
(Leroy et al. 2008, Bigiel et al. 2008)
Resolution: 750 pc

VLA: 21 cm -> HI
mm antennas: CO -> H2
Spitzer: 24 µm
GALEX: UV
24 µm + UV -> SFR

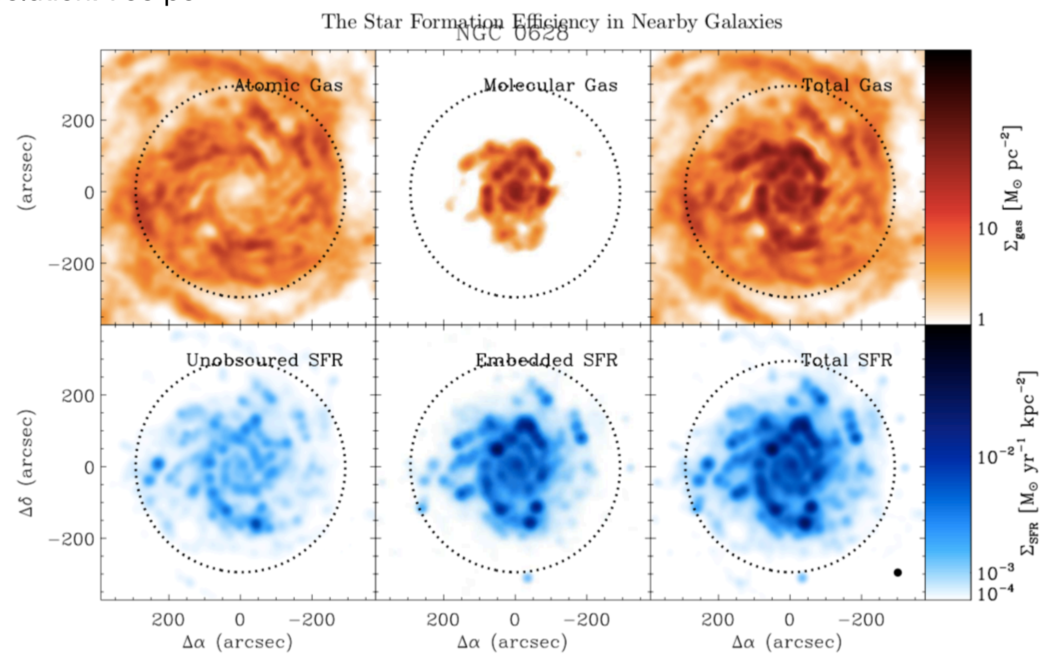

These images show, starting from upper left panel: atomic gas surface density measured from 21 cm, molecular gas surface density as traced by C-O, total gas surface density, SFR from Galex FUV data, obscured ("embedded") SFR from Spitzer 24 micron images, total SFR adding the two source.

The Schmidt-Kennicutt relation

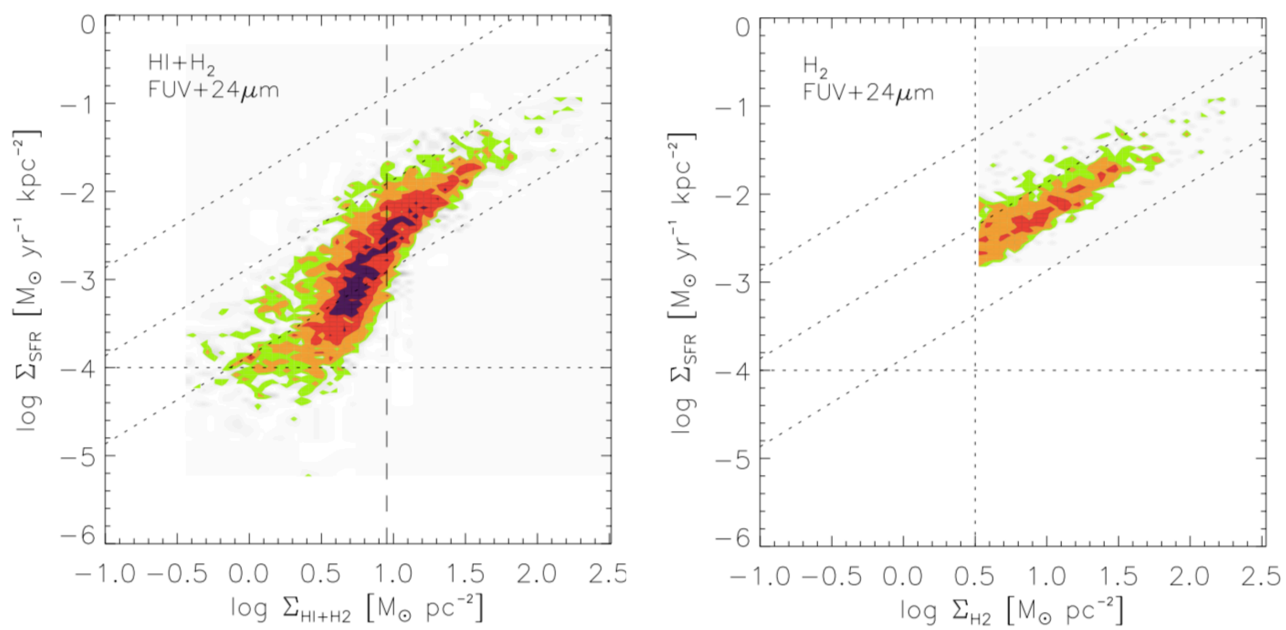

total gas: different regimes

molecular gas: linear relation

The SFR and gas surface densities are reported in this plot for many pixels (~750 pc x 750 pc) of a set of observed nearby galaxies, colors are darker where most pixels lie. The x-axis of these two plots reports, respectively, total gas surface density (left) and molecular gas surface density, the y-axis the SFR surface density.

The Schmidt-Kennicutt relation

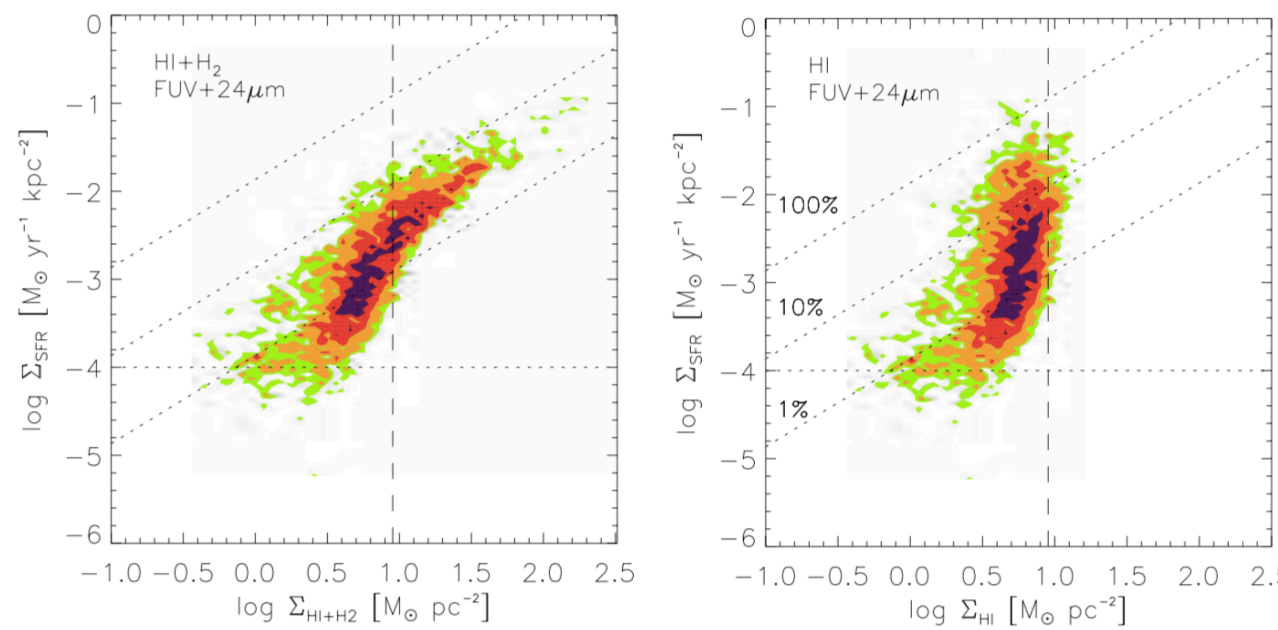

total gas: different regimes

neutral gas: no correlation

Here the right plot reports in the x-axis the neutral gas (21 cm) gas surface density. The conclusion is that neutral gas has only a poor correlation with SFR at very low surface densities, but molecular gas shows an almost linear correlation with SFR.

Timescales of star formation

Gas consumption timescale:

$$t_{\rm gc} = \Sigma_{\rm mol}/\Sigma_{\rm SFR} \simeq 2 \text{ Gyr}$$

Dynamical time of molecular clouds:

$$t_{\rm dyn} \simeq 20 \text{ Myr}$$

Fraction of stars formed per dynamical time:

$$f_\star \simeq 1 \ \%$$

Star formation rate:

$$SFR = f_\star M_{\rm mol}/t_{\rm dyn}$$

Then:

$$t_{\rm dyn} \simeq f_\star t_{\rm gc}$$

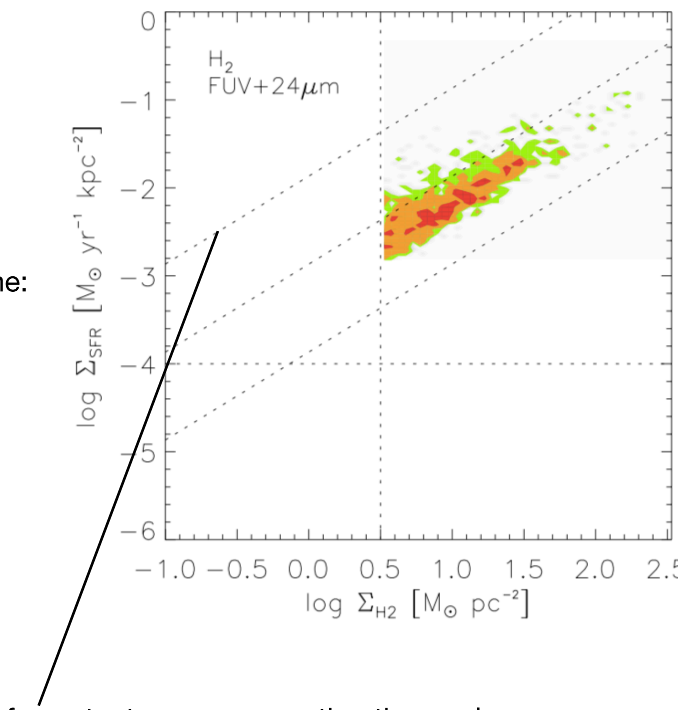

Lines of constant gas consumption timescale

We can define a gas consumption timescale (sometimes called efficiency of star formation) as the ratio between molecular gas and SFR surface densities (measured of course on the same pixel in the sky). This turns out to be ~2 Gyr in local spirals. We can compute the dynamical time of molecular clouds, that results to be ~20 Myr. A small fraction of the gas, ~1%, is transformed into stars at each dynamical time (the molecular cloud is destroyed by its massive stars, so it lasts just ~1-2 dynamical times). The SFR of a molecular cloud can be written as in the fourth equation, so f_star, t_dyn and t_gc are connected by the simple relation given in the last equation.

Passive and active galaxies

Below we discuss on how passive and active galaxies behave at low redshift.

The effect of cosmic expansion on galaxy SEDs

Cosmological redshift,
-> observed-frame vs rest-frame

$$\lambda_o = \lambda_e(1+z)$$

cosmological dimming,

$$I_\nu \propto (1+z)^{-4}$$

K-correction: magnitudes and colors must be corrected to recover rest-frame quantities; this correction depends on knowledge of the galaxy SED.

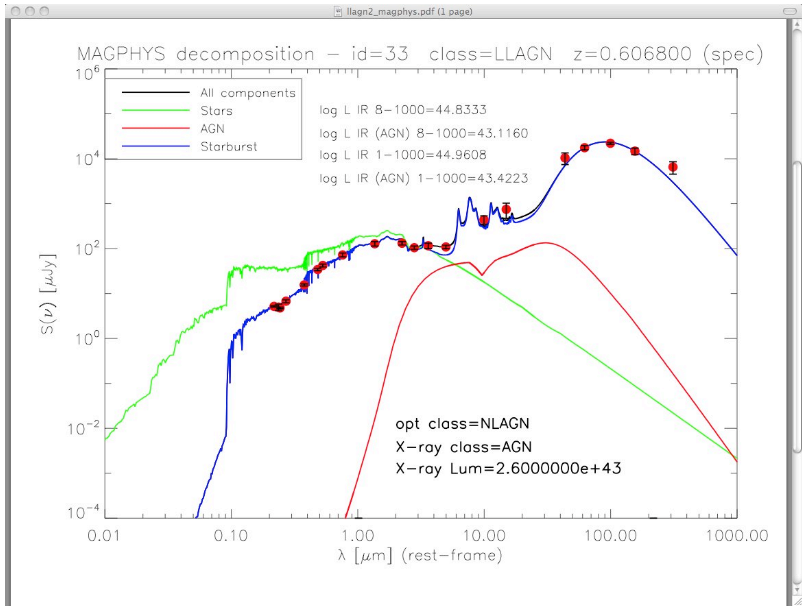

This slide discusses the main effects of cosmic expansion on galaxy SEDs.

Bimodality of the color-magnitude relation

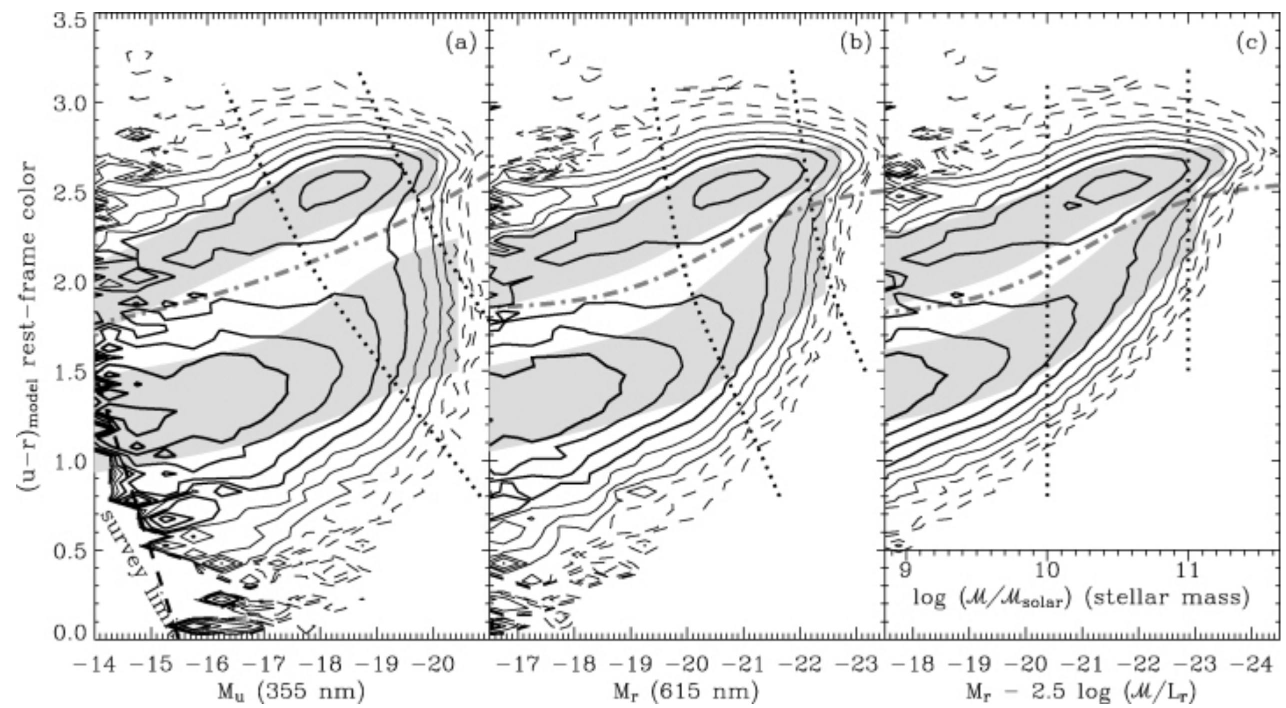

Baldry et al. (2006, MNRAS, 373, 469)

The Sloan Digital Sky Survey has been used to have high statistics for local galaxies. Here we show in the left and middle panels the color-magnitude relation of galaxies, where magnitudes and colors have been subject to K-correction; magnitudes are in u and r bands (in the ugriz system of SDSS), the color is u-r. The right panel shows the same plot using the measured stellar mass in the x-axis.

Bimodality of the color-magnitude relation

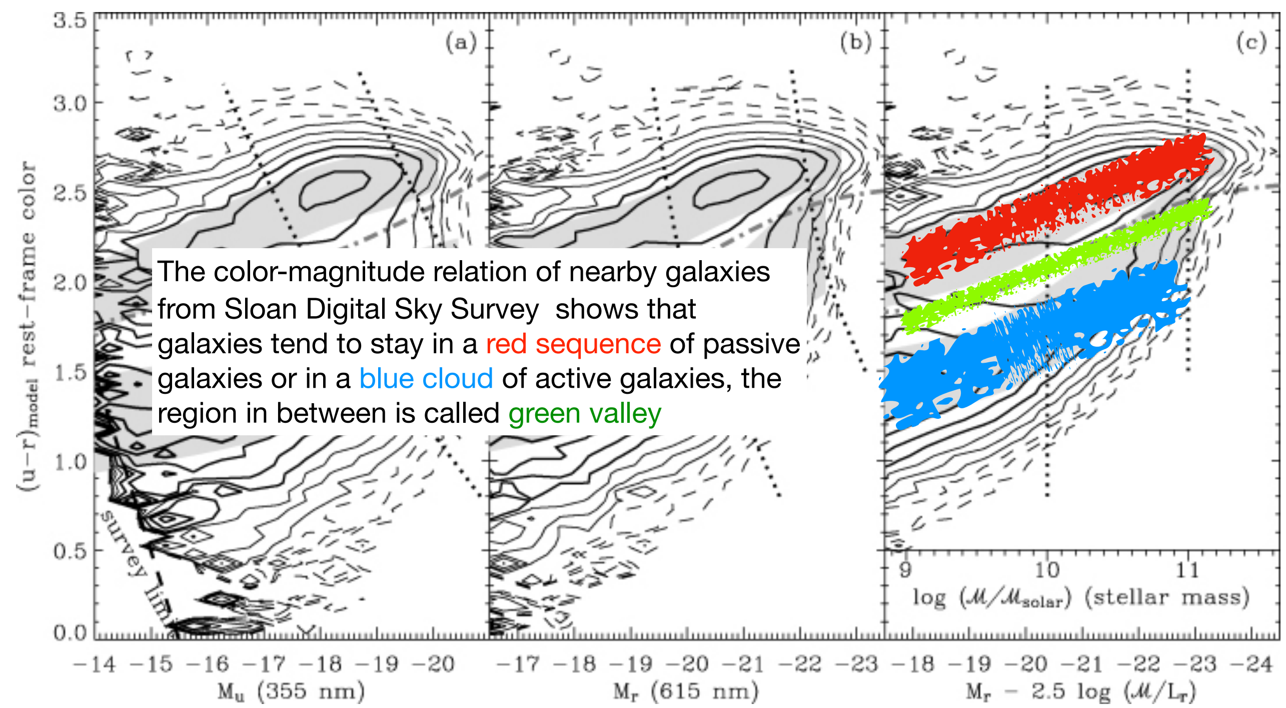

Baldry et al. (2006, MNRAS, 373, 469)

In this plot galaxies clearly tend to stay in two main regions, the red sequence (characteristic of galaxy clusters) and the blue cloud. Galaxies in the transition region are said to stay in the "green valley".

Selection of active and passive galaxies from rest-frame colors

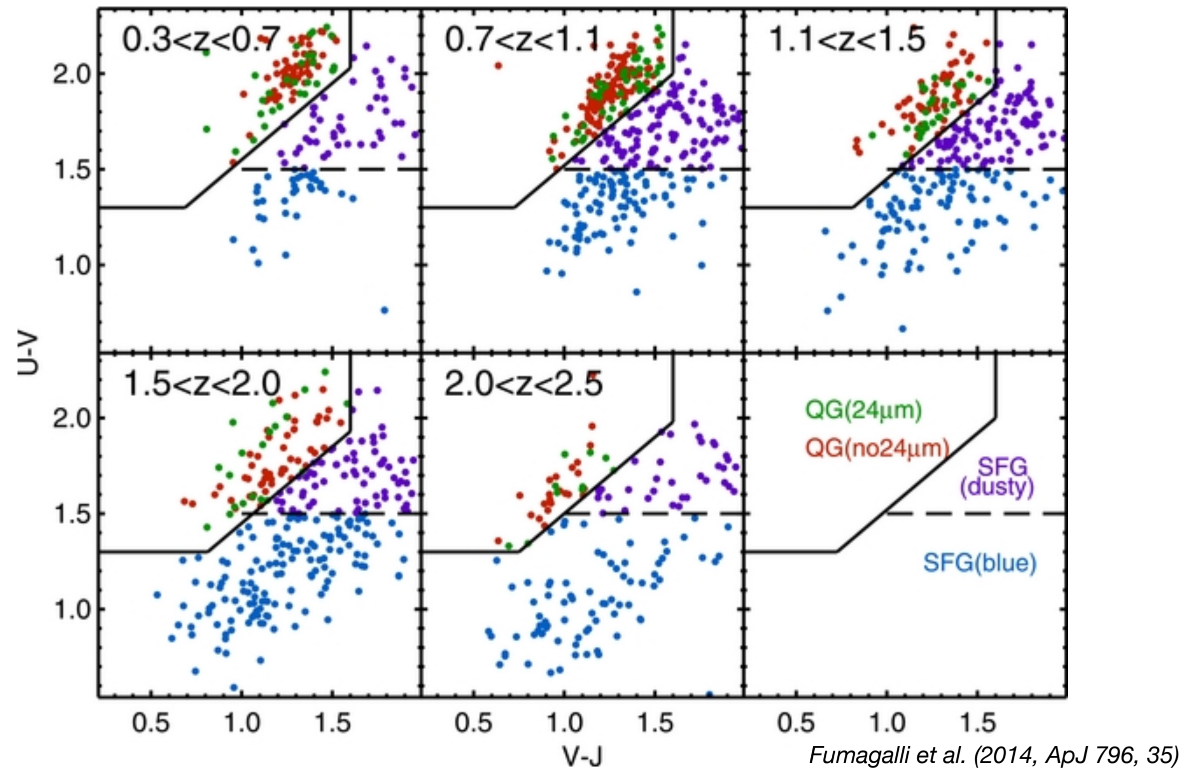

With sufficient sampling of the SED, rest-frame colors can be recovered and passive and active galaxies can be distinguished at any redshift. Clearly this distinction is subject to uncertainties, and will not exactly correspond to a distinction based on spectra (where emission lines reveal the presence of HII regions, and thus of star formation even for reddish galaxies). In the figure: QG=quiescent galaxies, SFG=star-forming galaxies.

Main sequence of star-forming galaxies

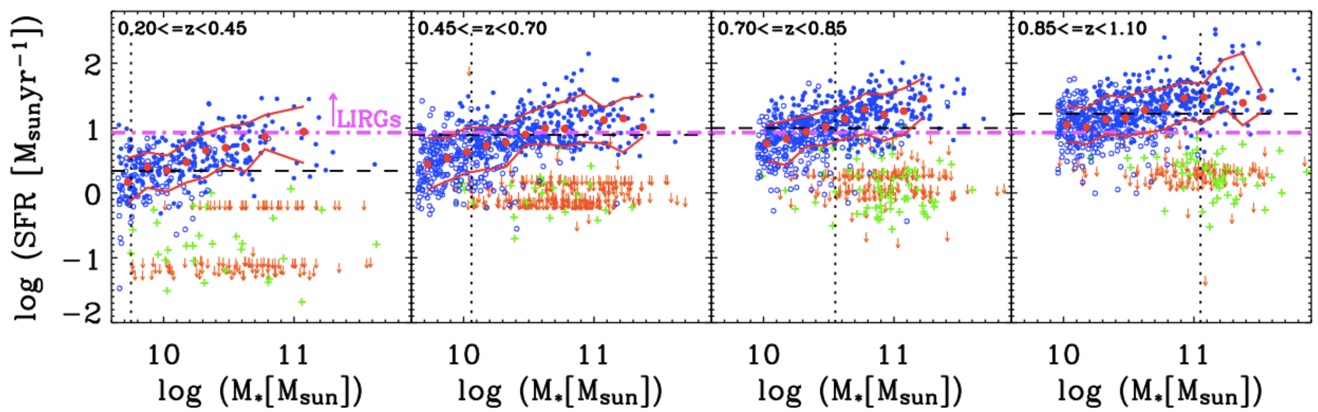

Noeske et al (2006)

$$SSFR = \frac{SFR}{M_\star}, \quad \mathrm{Gyr}^{-1}$$

$$\text{Passive galaxies : } SSFR < 10^{-11}\ \mathrm{Gyr}^{-1}$$

For star-forming galaxies, SFR and stellar mass are correlated, forming what is called the main sequence of star-forming galaxies. This allows us to define the Specific SFR, in units of 1/Gyr. The SSFR has this meaning: if the SFR is kept constant, stellar mass doubles in a time equal to SSFR^-1.

Potential biases in the main sequence

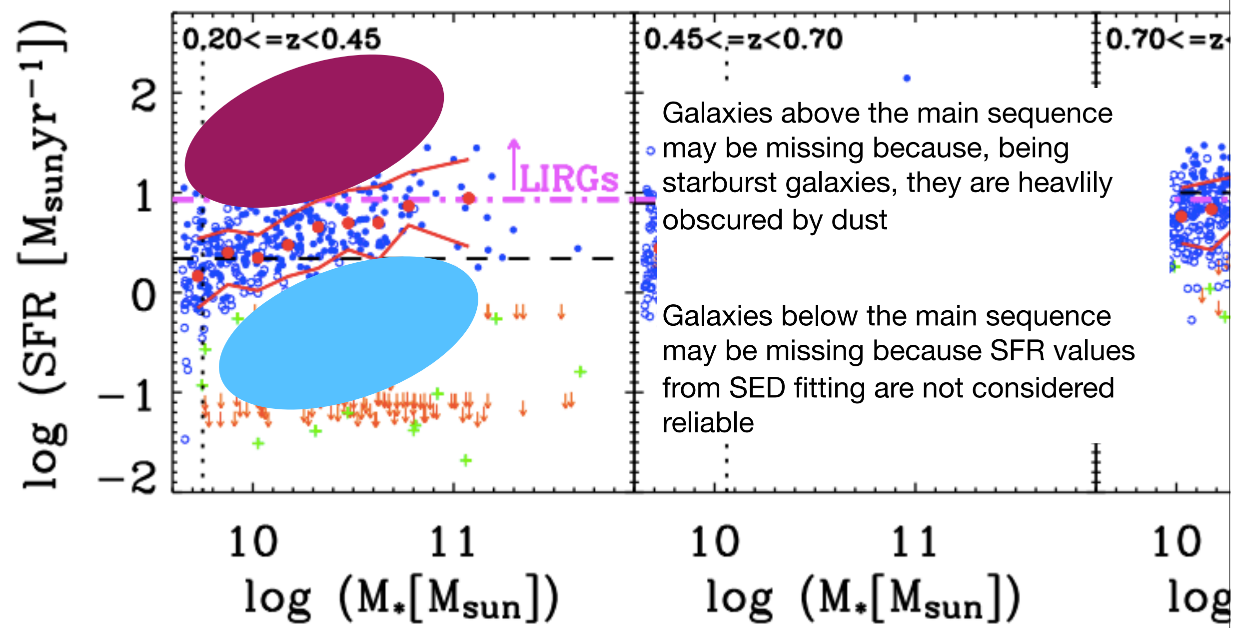

This slides illustrates why the main sequence could be seen tighter than what it intrinsically is, due to selection effects.

Observing galaxies at high redshift

Below we discuss the techniques needed to observe high-z galaxies.

Extragalactic surveys

Main properties:

Surveyed area on the sky
Observed bands
Depth in each band -> confusion limit
Target selection for spectroscopy
Spectroscopic redshifts
Photometric redshifts

To control systematics:

Completeness: fraction of galaxies really observed as a function of magnitude
Purity: fraction of objects that are true galaxies
Angular mask: completeness and purity maps on the sky
Spectroscopic redshift errors
Photometric redshift errors

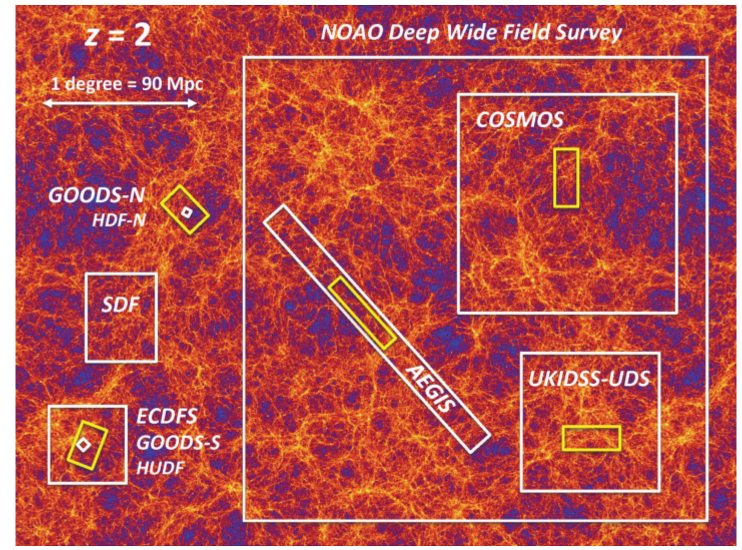

from Madau & Dickinson

This slide gives an overview of deep galaxy surveys used to investigate the nature of high-redshift galaxies. More details can be found in Madau & Dickinson.

Selection of high-redshift galaxies

Complete spectroscopic surveys of a deep field with Multi-Object Spectrographs:

just observe one small field, like the Hubble deep and ultra-deep fields, and take spectra for all the galaxies that are bright enough

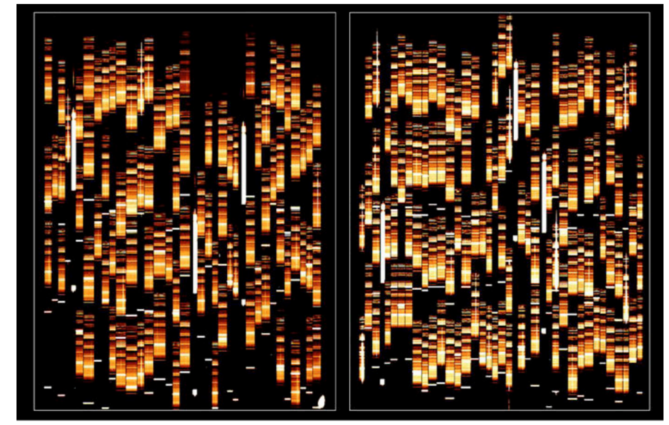

In this case a Multi-Object Spectrograph is neeeded, the image is taken with the VIMOS spectrograph at VLT, able to take ~1000 spectra for each observation.

Selection of high-redshift galaxies

Complete spectroscopic surveys of a deep field with Multi-Object Spectrographs;

Galaxies in massive galaxy clusters at z~1:

these systems can be recognized both as galaxy overdensities and as X-ray soures, galaxies in that field have a high probability of belonging to the cluster

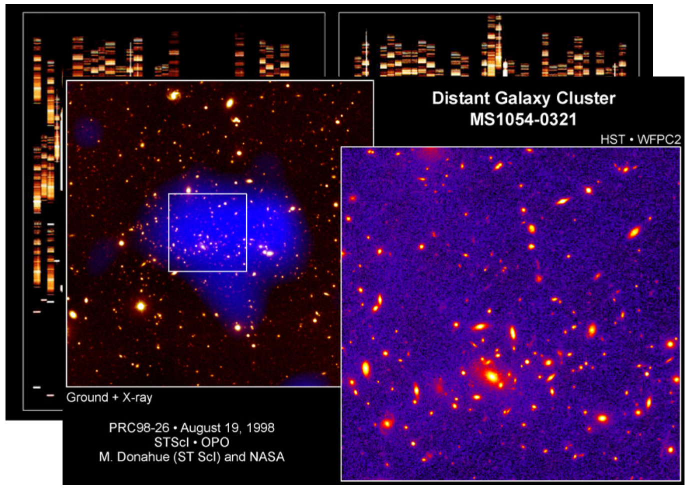

Moreover, galaxies in the cluster core are mostly ellipticals, so they trace a very neat red sequence in the color-magnitude diagram that can be used to ease their recognition.

Selection of high-redshift galaxies

Complete spectroscopic surveys of a deep field with Multi-Object Spectrographs;

Galaxies in massive galaxy clusters at z~1;

photometric redshifts from SED fitting:

redshift is one of the crucial parameters for SED fitting, even few bands are sufficient to obtain a redshift determination

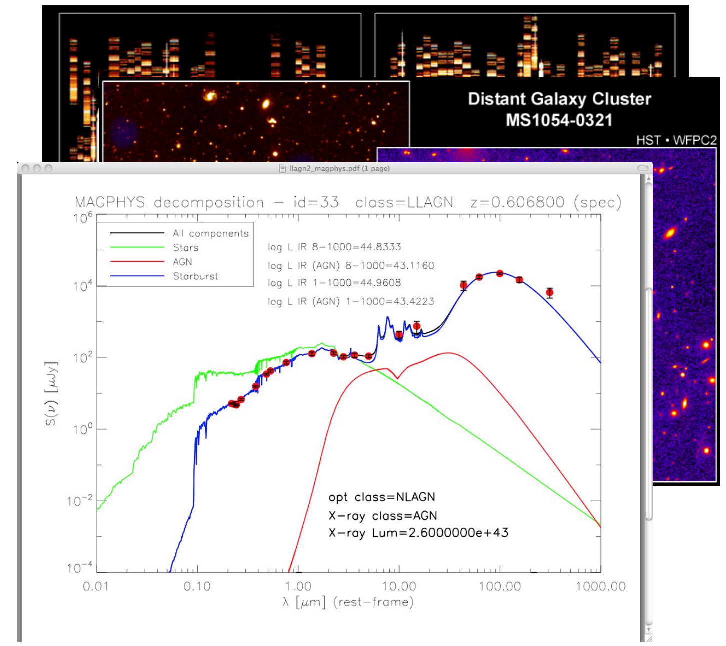

A great effort is devoted to photometric redshift, because, trained on a limited set of spectroscopic redshifts, they give the possibility to have redshifts for large galaxy samples.

Selection of

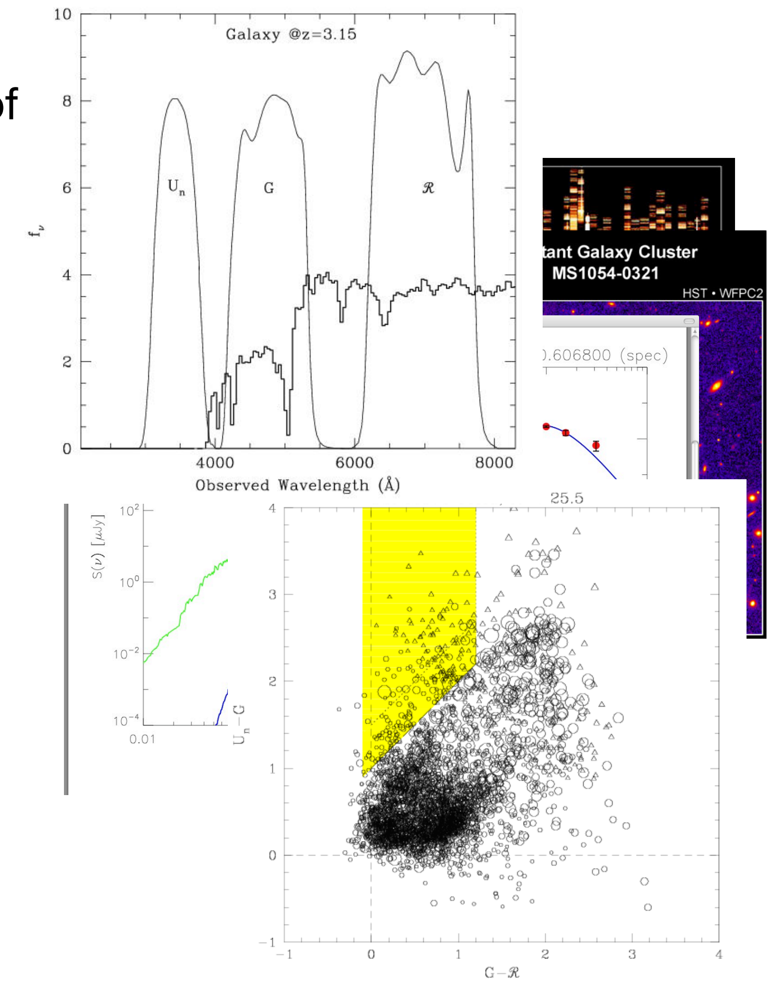

Complete spectroscopic surveys of a deep field with Multi-Object Spectrographs;

Galaxies in massive galaxy clusters at z~1;

photometric redshifts from SED fitting;

Lyman-break galaxies:

at high redshift the Lyman break enters optical or NUV filters, galaxies then "drop out" of blue images and their colors are easily recognisable

The Lyman-break technique is probably the most effective way to select distant galaxies with much neutral hydrogen; this is generally true for star-forming galaxies. However, a sample of Lyman-break galaxies has a high purity, making it ideal for spectroscopic follow-up, but not necessarily a high completeness, meaning that some star-forming galaxies may be missed. For sure, passive galaxies are not selected by this technique.

Selection of high-redshift galaxies

Complete spectroscopic surveys of a deep field with Multi-Object Spectrographs;

Galaxies in massive galaxy clusters at z~1;

photometric redshifts from SED fitting;

Lyman-break galaxies;

other color-color techniques (BzK):

star-forming or passive galaxies at z~1.5 acquire recognizable colors due to their redshift.

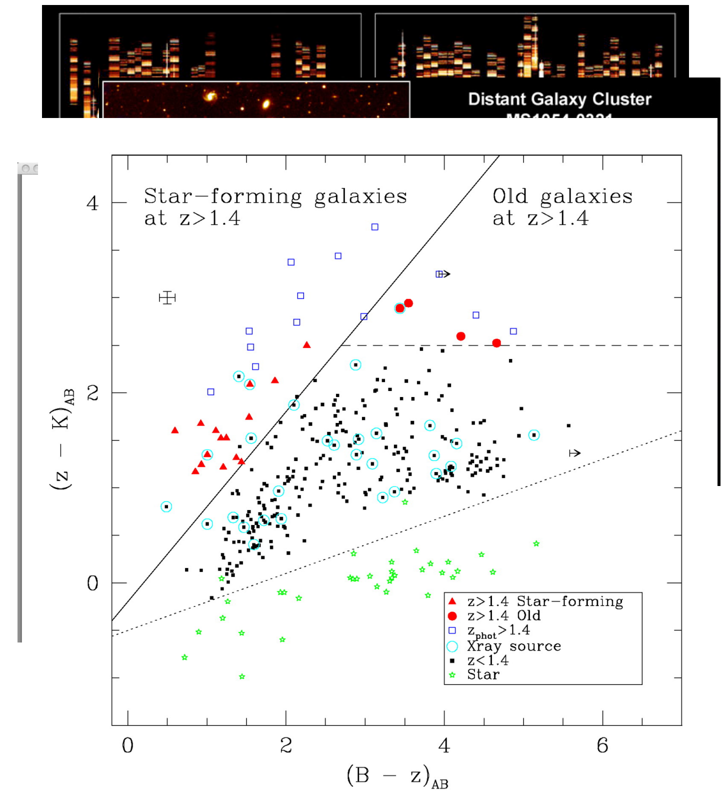

The BzK technique is based on observed-frame colors, and allows to effectively select both passive and star-forming galaxies at z~1.5-2, where the Lyman break is still in the FUV and so the Lyman break technique is less effective. This region has been called "redshift desert" for some time.

Selection of high-redshift galaxies

Complete spectroscopic surveys of a deep field with Multi-Object Spectrographs;

Galaxies in massive galaxy clusters at z~1;

photometric redshifts from SED fitting;

Lyman-break galaxies;

other color-color techniques (BzK);

Lyman-alpha emitters:

observations with a narrow filter can reveal galaxies that have a strong Lyman alpha emission line.

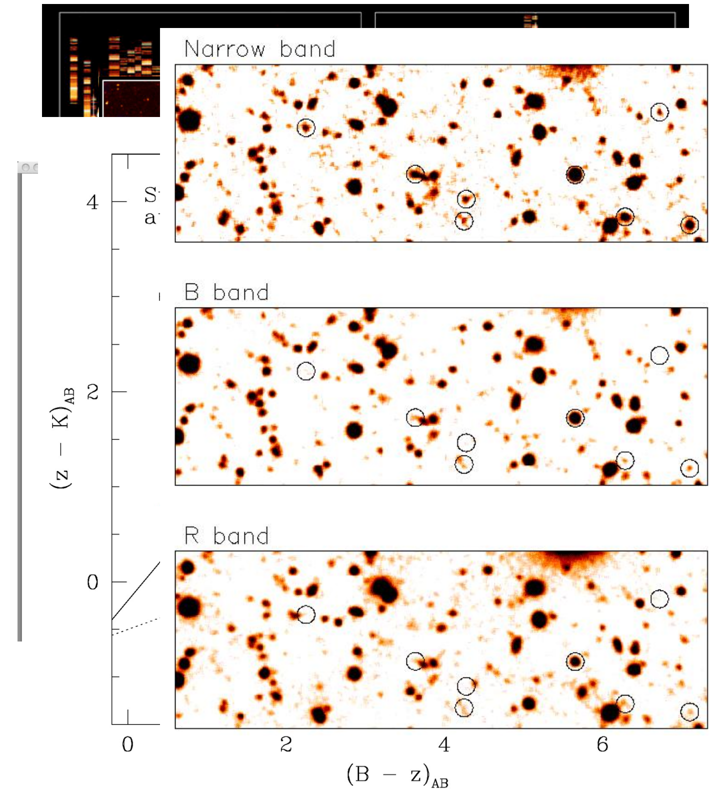

A narrow filter will highlight galaxies that have a strong emission line just entering the filter. However, Lyman-alpha could be confused with, say, [OII] from a lower-redshift galaxy. A high purity is obtained by taking images in filters before and after the narrow filter; a Lyman-alpha galaxy should be faint in the blued band, due to the Lyman break.

Selection of high-redshift galaxies

Complete spectroscopic surveys of a deep field with Multi-Object Spectrographs;

Galaxies in massive galaxy clusters a z~1;

photometric redshifts from SED fitting

Lyman-break galaxies;

other color-color techniques (BzK);

Lyman-alpha emitters;

sub-mm galaxies:

the large positive K-correction at such long wavelenghts allows us to observe dusty star-forming galaxies in the sub-mm to very high redshift.

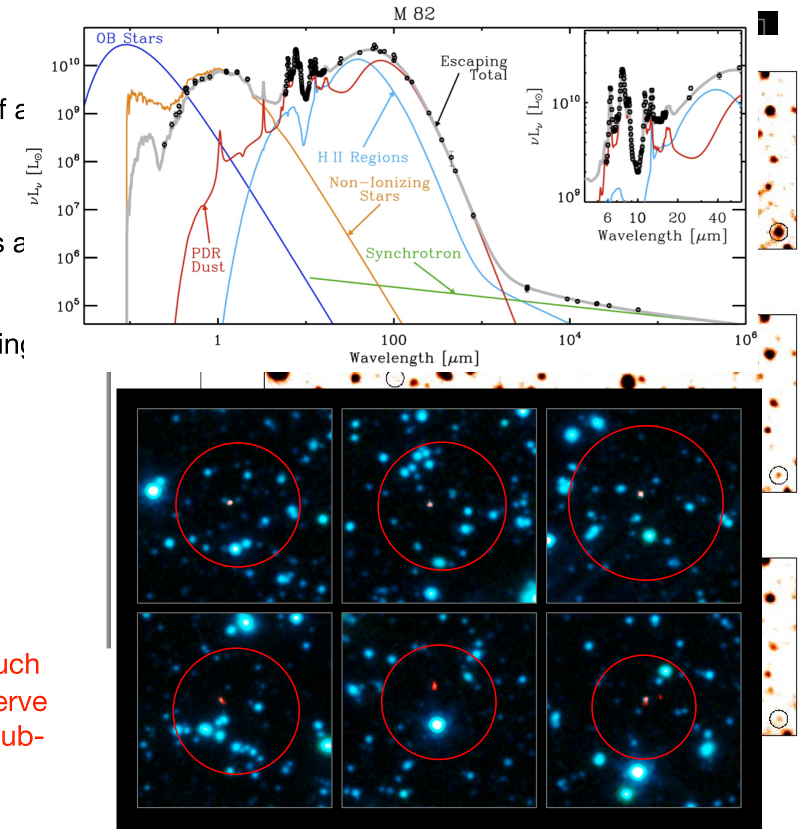

K correction in the FIR is positive, so galaxies in the sub-mm have fluxes that are roughly independent of distance (more distant objects are observed at rest-frame wavelengths nearer to the FIR peak). The image shows six fields (blue gives an optical image) centered on bright sub-mm sources; the red circle gives the position of the sources obtained using a single dish, the red dot is obtained with ALMA interferometer. The huge leap in angular resolution is evident.
Notice also that bright sub-mm sources are faint in the optical, they correspond to highly extincted galaxies.

Selection of high-redshift galaxies

Complete spectroscopic surveys of a deep field with Multi-Object Spectrographs;

Galaxies in massive galaxy clusters at z~1;

photometric redshifts from SED fitting;

Lyman-break galaxies;

other color-color techniques (BzK)

Lyman-alpha emitters;

sub-mm galaxies;

gravitational lenses:

high-redshift galaxies can be observed, highly amplified by lensing, in as background sources of clusters.

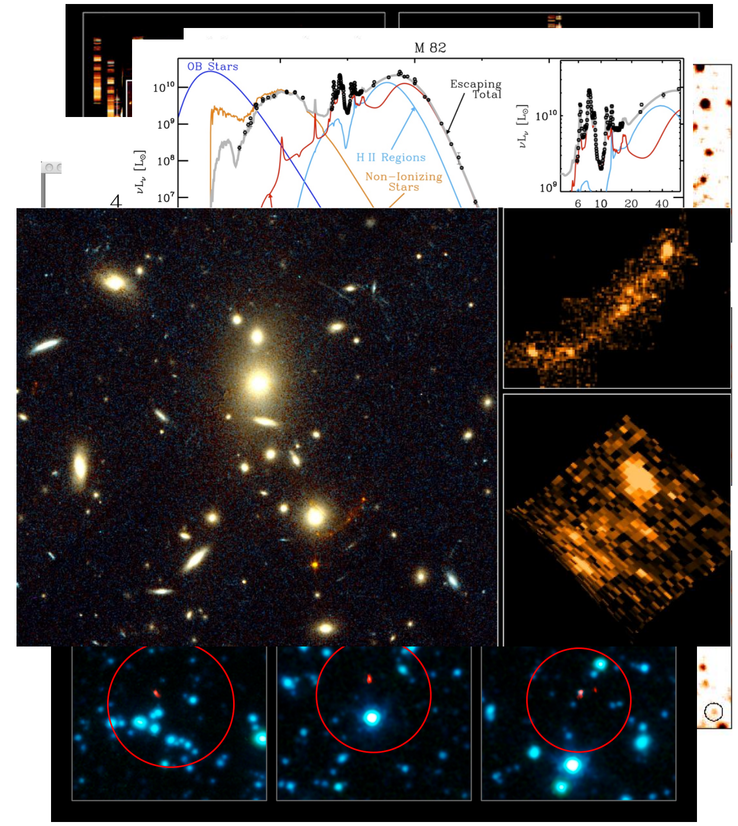

This is the image of a galaxy cluster with a highly distorted background galaxy. The right panels give a zoom of the lensed galaxy and a reconstruction of its de-lensed image.

On lensing: Refsdal supernova

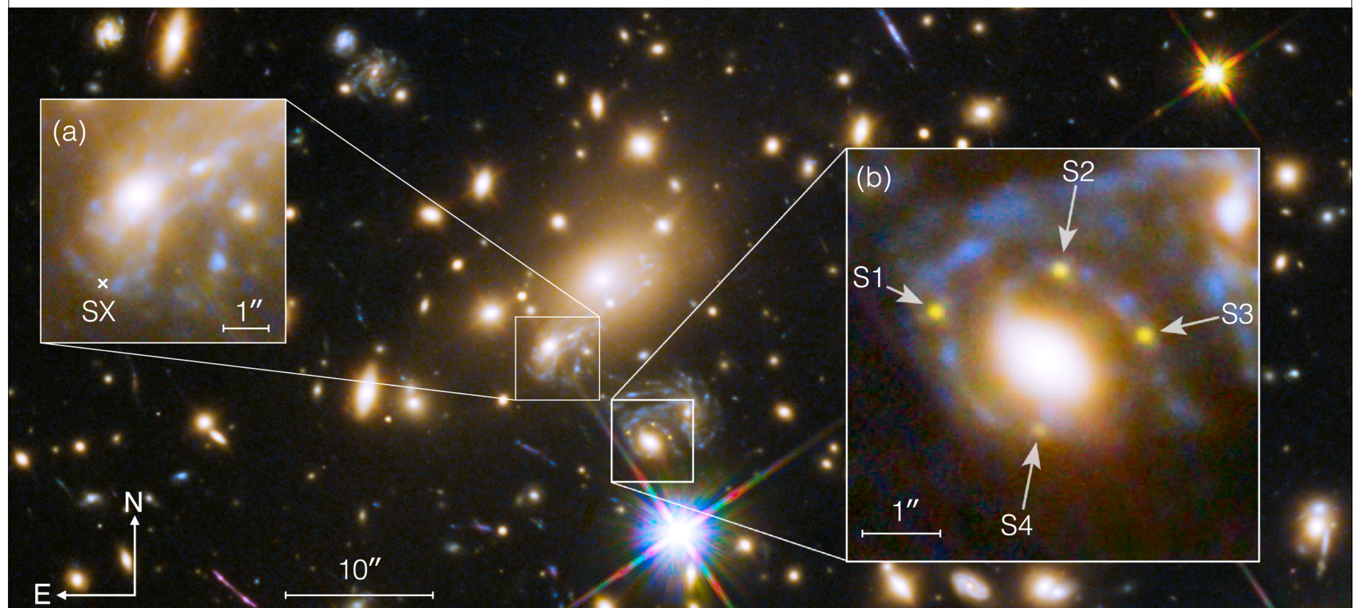

Grillo et al 2018 ApJ 860 94

A parenthesis on lensing: if a SN is found in a lensed galaxy, the timing of the appearance of different images can be used to test lensing models, and in principle to measure the Hubble constant.

Evolution of stellar masses and SFRs

We now quantify the evolution of stellar masses and SFRs along the cosmic history.

Evolution of the rest-frame UV luminosity function

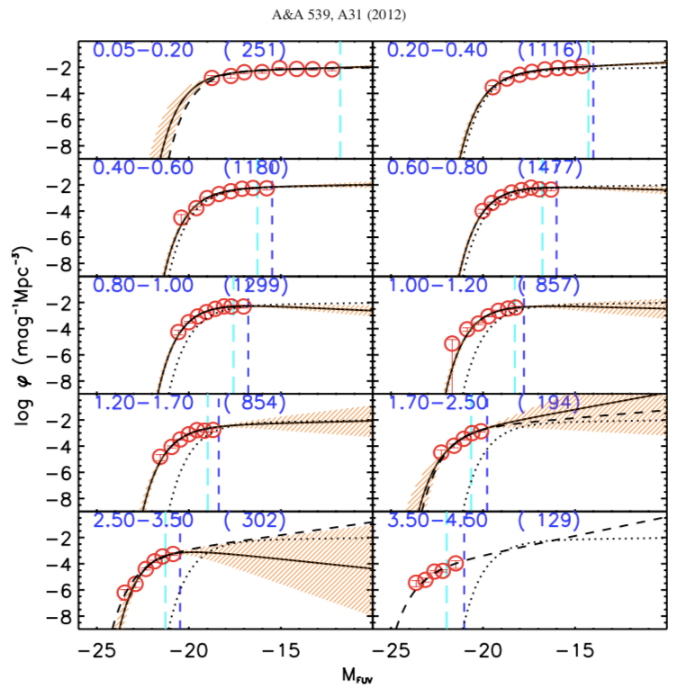

Cucciati et al. (2012)

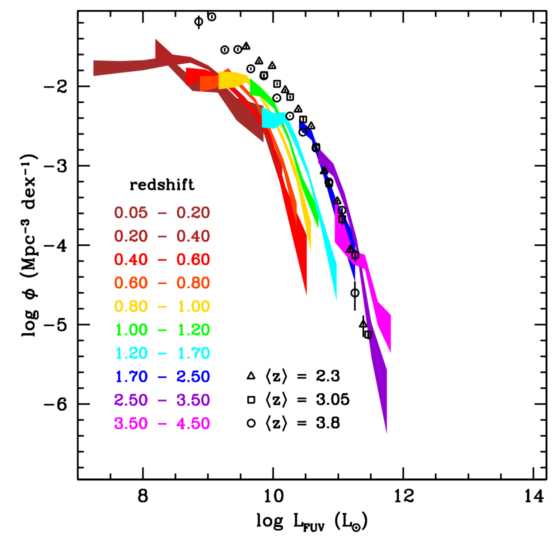

from Madau & Dickinson

Evolution of the rest-frame UV luminosity function

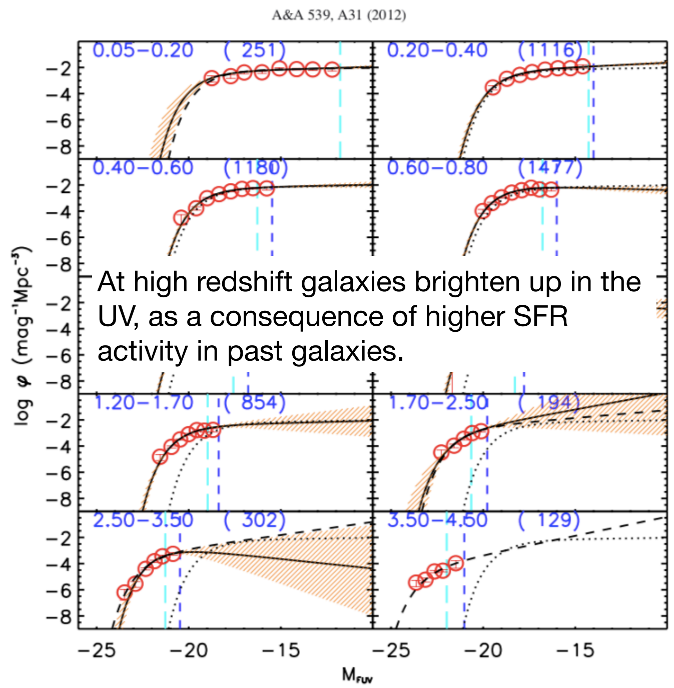

At high redshift galaxies brighten up in the UV, as a consequence of higher SFR activity in past galaxies.

Cucciati et al. (2012)

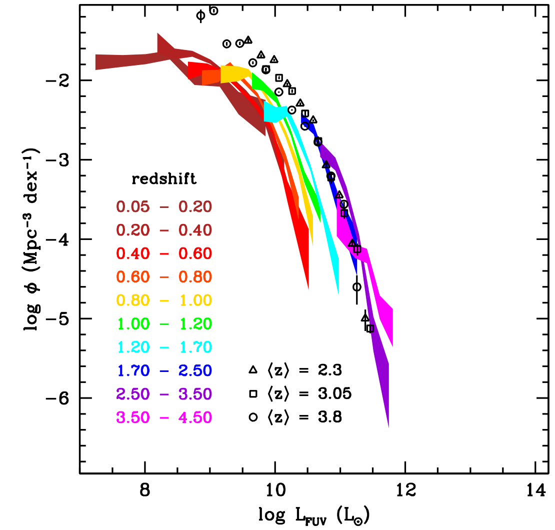

from Madau & Dickinson

The UV galaxy luminosity function shows that galaxies were brighter in the past.

Evolution of the total IR luminosity function

The same is observed in the IR, that however does not go deep enough to see faint galaxies at high redshift

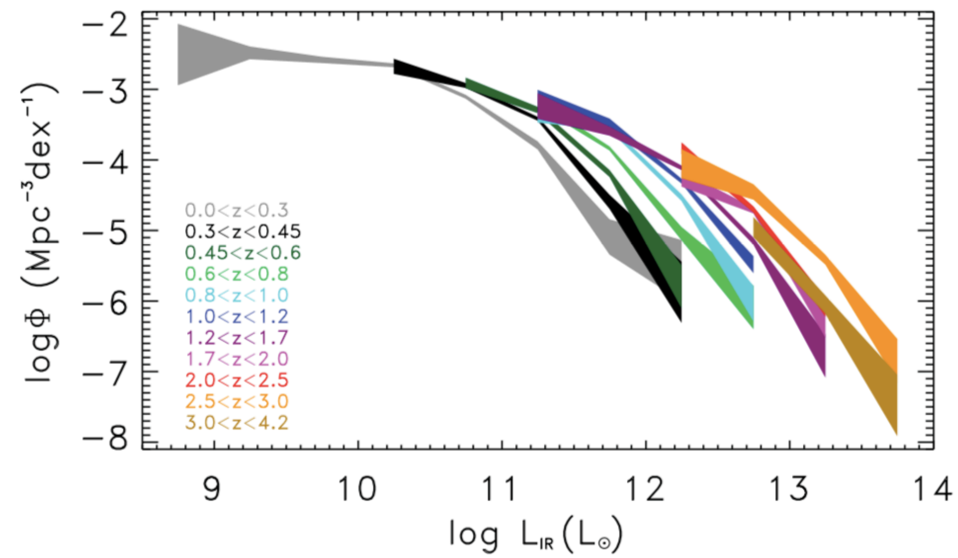

Gruppioni et al. (2013)

The brightening is confirmed by the FIR LF seen by Herschel, though it does not go deeper than the knee at z>=2, and cannot reach the highest redshifts.

Very high redshift galaxies

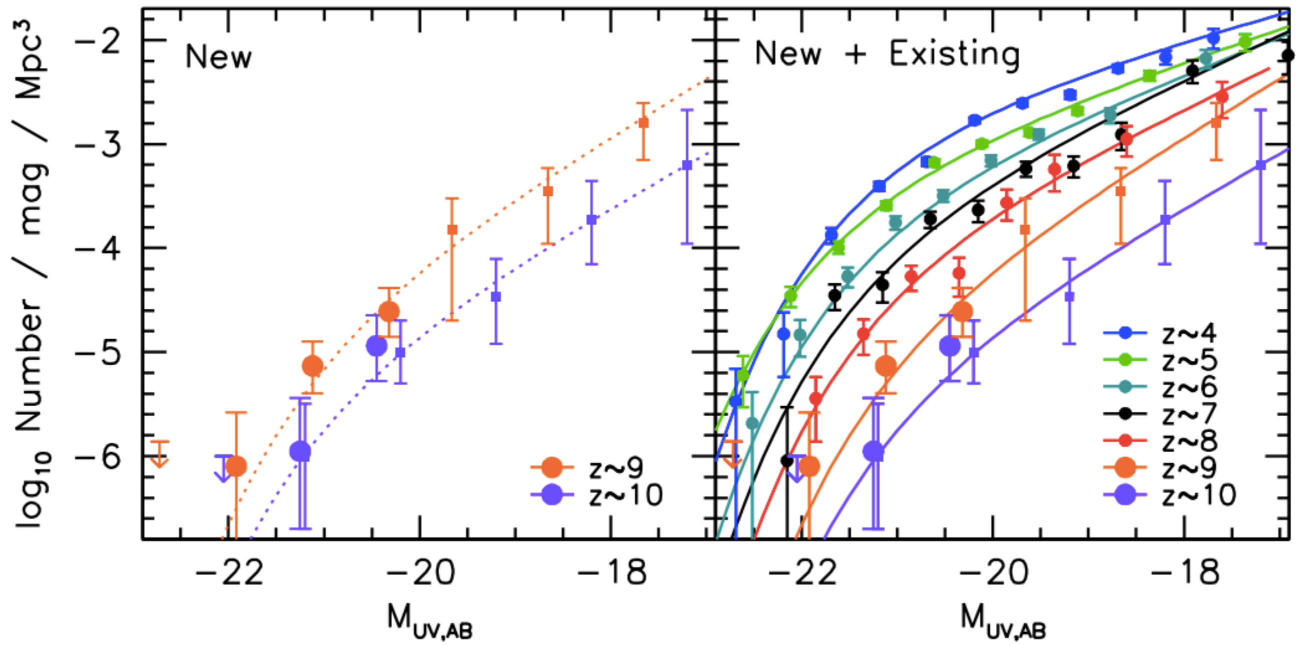

Bouwens et al. 2019, arXiv:1905.05202

Using the Lyman-break technique, one can produce reliable lists of candidate galaxies at very high redshift (4<z<10). Sometimes the luminosity functions are given even before spectroscopic confirmation of the candidates. Gravitational lensing allows to probe the low-luminosity tail of the FUV LF, though with uncertainties due to the lensing model. At the highest redshift we observe a dimming of galaxies, going toward higher redshift.

Evolution of galaxy (gas) metallicities

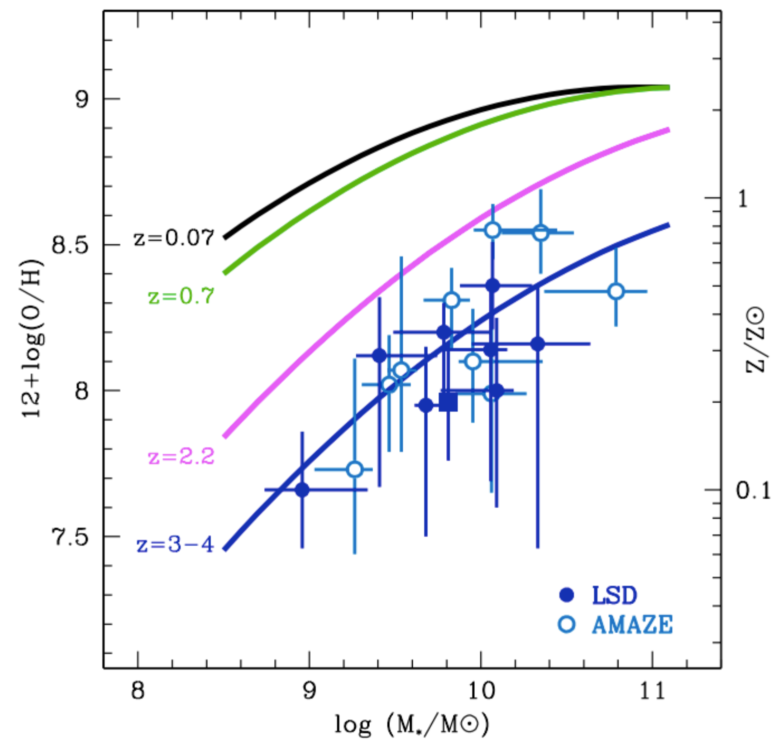

Mannucci & Cresci, arXiv:1011.0264

Measures of gas metallicities show evolution: galaxies at high redshift were less metallic.

Evolution of stellar mass function

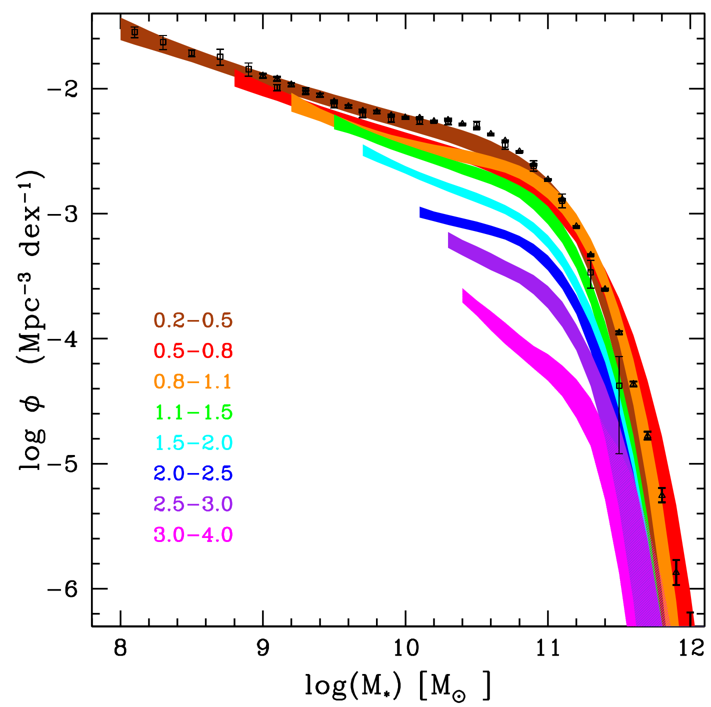

from Madau & Dickinson

Stellar mass function in several redshift bins, as computed from several surveys that span the whole cosmic history.

Evolution of SFR function

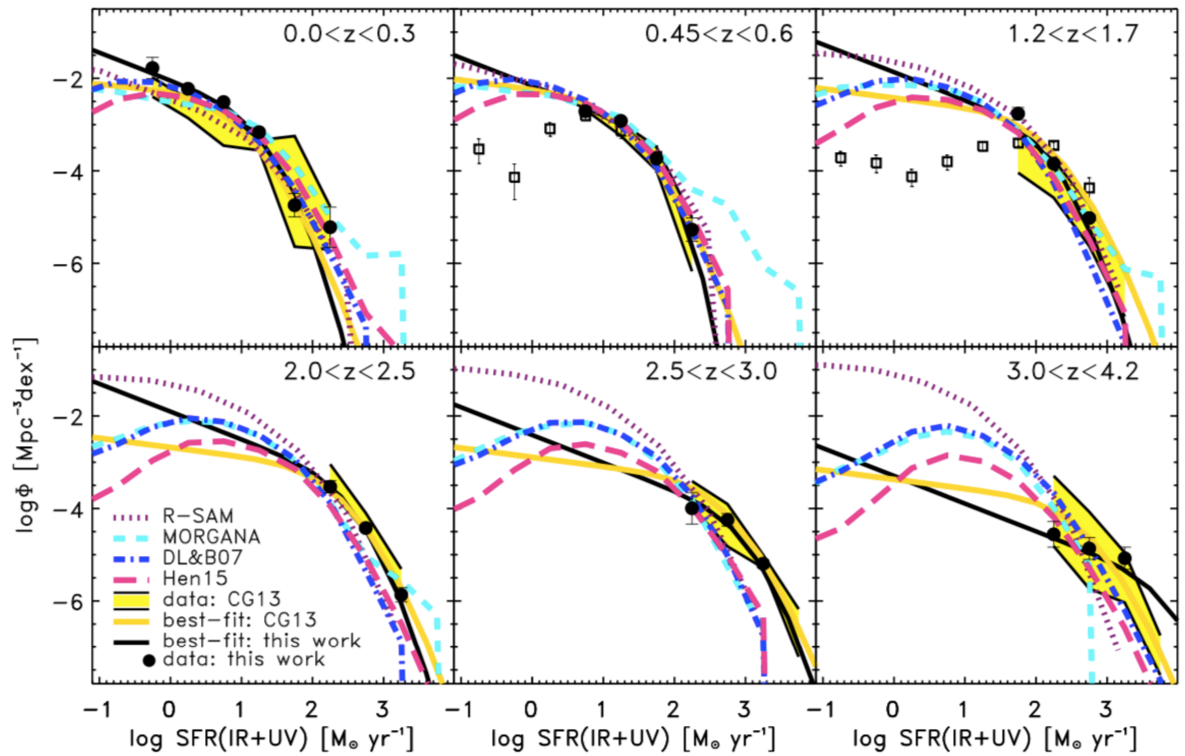

Gruppioni et al. (2015)

This is the star formation rate function, obtained from Herschel data, subtracting the AGN component. It is compared with models of galaxy formation, that are beyond our interest.

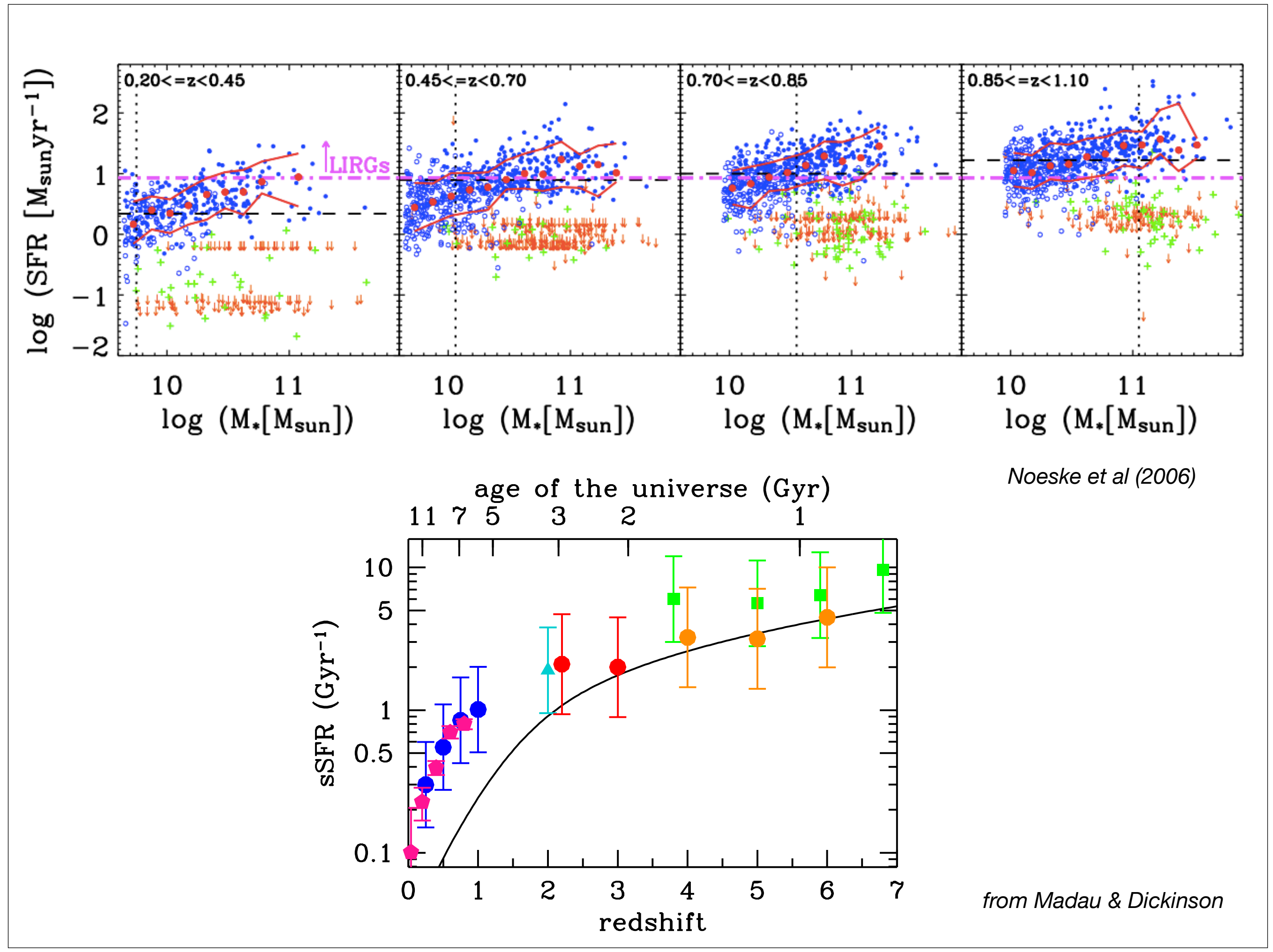

This figure shows that the main sequence of star-forming galaxies evolves in time. The lower panel shows the average SSFR of galaxies as a function of redshift. The main sequence grows by more than a factor of 10 to z~2, then the growth continues with a weaker trend.

The cosmic star formation history - UV and IR

$$LD(z) = \int_{L_{\min}}^{\infty} L\Phi(L;z)dL$$

$$\psi(z) = \kappa\, LD(z)$$
$$= \kappa_{\rm FUV}\, LD_{\rm FUV}(z)$$
$$+ \kappa_{\rm IR}\, LD_{\rm IR}(z)$$

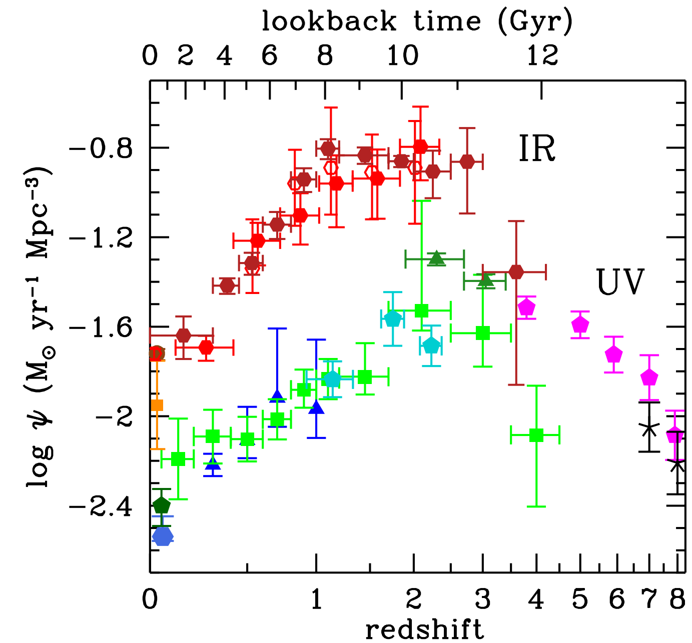

from Madau & Dickinson

Cosmic star formation history: SFR density of galaxies as a function of redshift. It is computed from the galaxy luminosity densities in FUV and IR, obtained by integrating the redshift-dependent LFs. The UV SFR density is related to the unextincted light, the IR one to the extincted light.

The cosmic star formation history

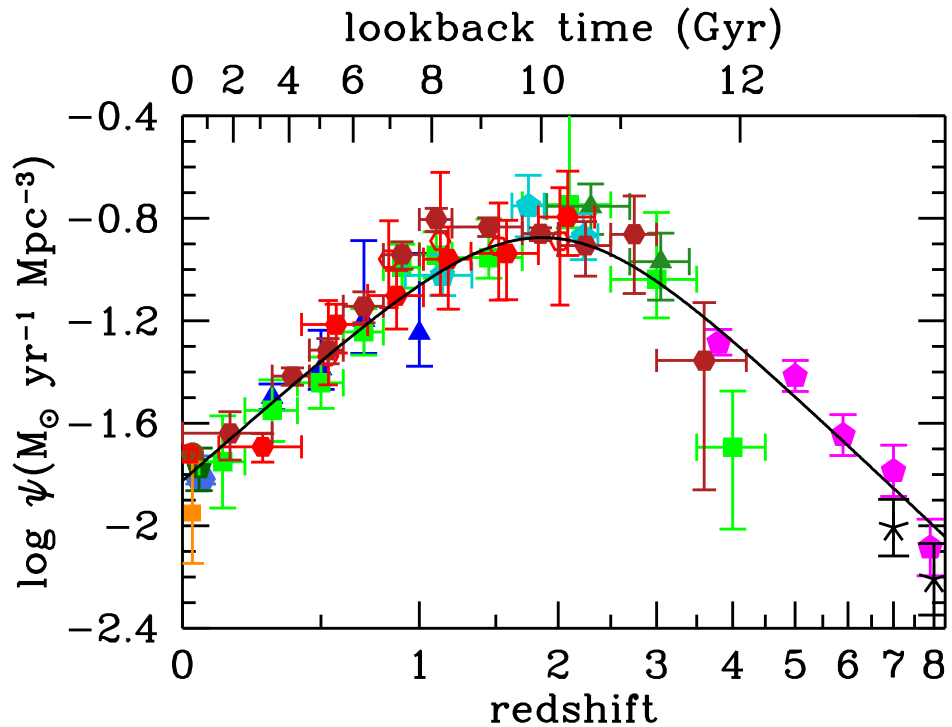

from Madau & Dickinson

This is obtained by summing the two relations obtained above. The black line is a fit.

This plot shows that the build-up of galaxies took place in the past, with the peak of activity at z~2, 10 Gyr ago.

The stellar mass density

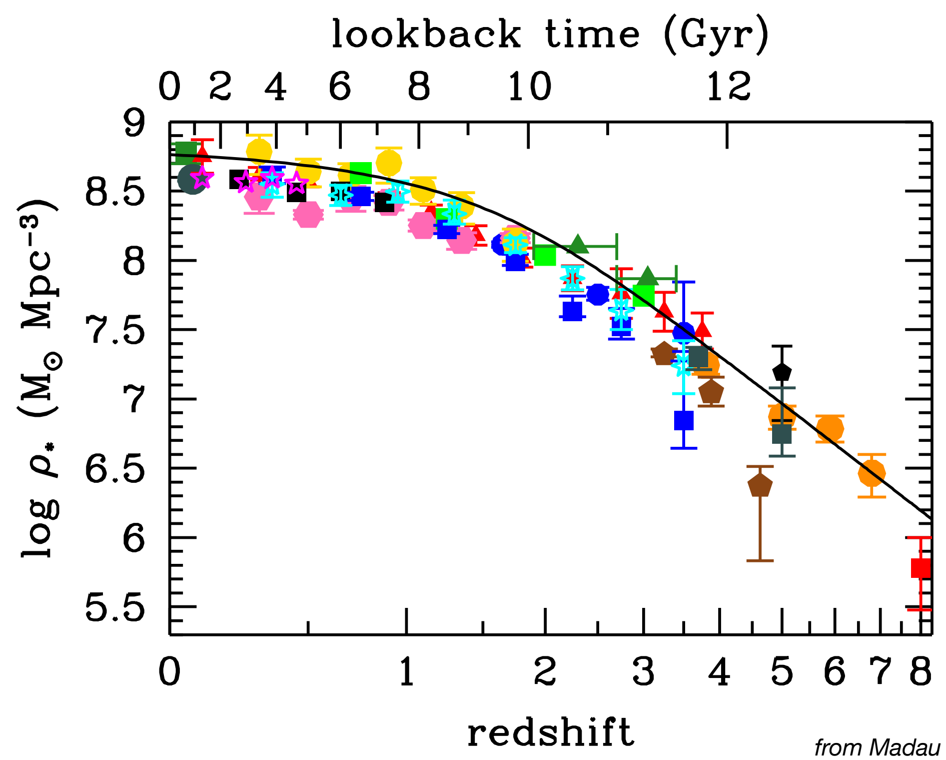

from Madau & Dickinson

Cosmic growth of stellar mass density. The black line is obtained by integrating the SFR(t) density, taking into account its evolution due to both star formation and death of stars more massive than ~1 solar mass. Consistency of the two curves is a good test of the validity of the assumptions made to obtain the two quantities - SFRs and stellar masses.

Ratio of IR and UV luminosity densities

$$LD = \int_{L_{\min}}^{\infty} L\Phi(L)dL$$

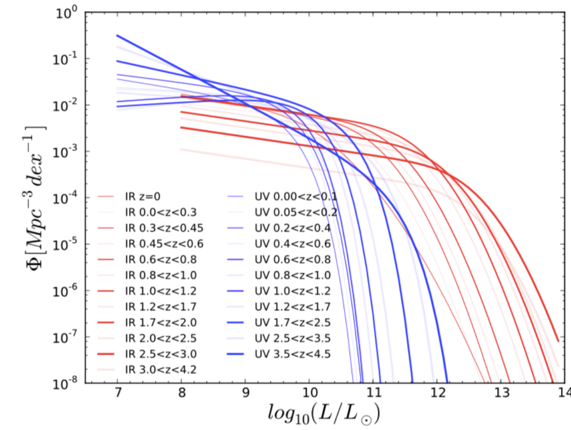

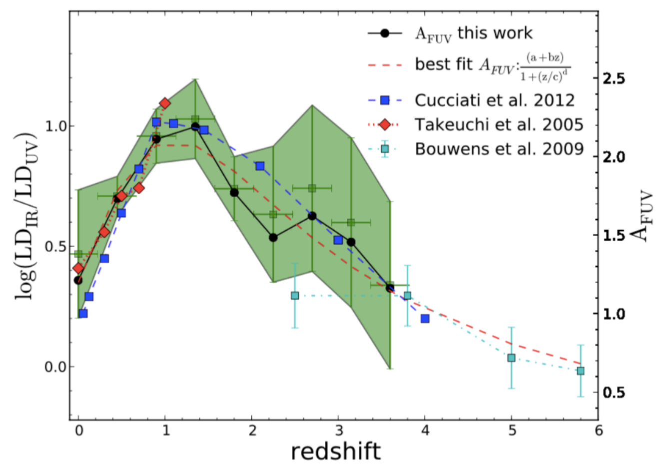

From the luminosity functions, one can compute the luminosity density of observed galaxies in the UV and IR; its ratio is a proxy of how dust extinction evolves with cosmic time.

Burgarella et al. (2013, A&A 554, A70)

Dust extinction seems to peak at z~1, consistent with the gradual accumulation of metals. This implies that extinction in high redshift galaxies should be less strong - though heavily obscrured galaxies exist at high redshift.